CONTENTS

PREFACE

The field of hydrology is of fundamental importance to civil and environmental engineers, hydraulic engineers, hydrogeologists, and other earth scientists because of the overall significance of water in modern society. Topics include water supply, major floods, droughts and their management, urban drainage and stormwater issues, floodplain management, climate change, and water quality impacts. In recent years, hurricanes and storm surge have caused significant coastal disasters, especially in coastal areas where urban development has expanded rapidly. This book was written to address the computational emphasis of modern hydrology both at an undergraduate and graduate level, and to provide a balanced approach in terms of theory and important applications in hydrologic engineering and science. A particular emphasis in the sixth edition is the incorporation of new examples, homework, and computer modeling applications.

THE EVOLUTION OF HYDROLOGY

Increasing use and sophistication of computer software and the accessibility of large-scale data have revolutionized the daily practice of hydrology. The impact of transferring online data from governmental and scientific sources to the practicing hydrologist or student has been phenomenal. Hydrologic rainfall data, digital terrain models, and mapping software linked with hydrologic modeling now allow complex problems to be solved efficiently. Geographical information systems (GIS) and radar rainfall have greatly improved our ability to predict hydrologic response. A number of major improvements have been made to existing hydrologic models, such as HEC-HMS, HEC-RAS, and EPA SWMM. These advances are highlighted with examples in the sixth edition. Important websites and links currently used routinely in hydrology are listed in Appendix E and can also be found at the textbook website: **hydrology.rice.edu**. While the entire textbook was updated with many new examples and new homework problems, the following lists the most important updates incorporated for the sixth edition.

- Chapter 6: New SWMM5 example embedded in a real case study of the application of decentralized stormwater controls
- Chapter 7: New HEC-RAS discussion with a new detailed example
- Chapter 8: New examples in groundwater modeling
- Chapter 10: New chapter on GIS in Hydrology with a new example
- Chapter 11: Completely updated and includes new V*flo*® example

- Chapter 12: New chapter highlighting flood policy evolution in the United States.
- Chapter 13: New chapter on water resources case studies across America.

ORGANIZATION OF THE SIXTH EDITION

The sixth edition of the text is still divided into three main sections. **The first section**, consisting of the first four chapters, covers traditional topics in hydrology related to the water balance such as: (1) hydrologic principles, hydrologic cycle, and measurement techniques, (2) hydrologic analysis using hydrographs for rainfall-runoff, (3) statistical and flood frequency analysis, and (4) hydrologic and hydraulic flood routing methods. These chapters provide a lot of the basis for more applied modeling applications in later chapters of the text. Many new figures, examples, and homework problems have been included throughout.

The second major section, Chapters 5 through 9, is designed to apply hydrologic theory and available hydrologic modeling techniques to several areas of engineering hydrology and design: watershed analysis, floodplain delineation, urban stormwater, ground water, and drainage design. The latest methods and computer models are described in enough detail for practical use. Updated examples and new case studies are also provided. Chapter 5, Hydrologic Simulation Models, has been updated to include the latest versions of the HEC-HMS model. Chapter 6, Urban Hydrology, presents methods and reviews of available computer models for pipe and open channel storm drainage systems. The Storm Water Management Model (SWMM5) is highlighted with a new watershed planning example. Chapter 7, Floodplain Hydraulics, first covers open channel flow concepts, including uniform flow and critical flow. These concepts form the basis for various hydraulic analyses such as water surface profile computations in a hydraulic model, HEC-RAS, described in detail with a new case study demonstrating the power of the model in steady and unsteady mode to evaluate natural floodplains. Chapter 8 presents ground water hydrology as a stand-alone chapter, including flow in porous media, aquifer properties, well mechanics, and computer applications. Governing equations of flow are derived and applied to a number of ground water problems, and a new example has been added. Chapter 9 is a comprehensive chapter on design applications in hydrology. It addresses design rainfall, small watershed design, hydraulic design, detention pond design, detailed culvert design, and floodplain mitigation design issues.

The final major section includes four chapters (10, 11, 12, and 13) that have been completely redone to cover a variety of interesting and relevant topics such as GIS data analysis and hydrologic computation, radar rainfall and watershed evaluation, severe storm impacts and flood management, and water resource case studies from across the United

States. No other hydrology textbook presents this type of material all in one place. Chapter 10 presents current geographic information systems (GISs) and digital elevation models (DEMs) as important tools for watershed and land use analysis, hydrologic modeling, and advanced floodplain delineation. Many useful hydrologic datasets and software are now widely available in high-resolution digital form on the web (see Appendix E). Chapter 11 depicts some of the latest technology on the use of NEXRAD radar data to estimate rainfall intensities over watershed areas. Radar rainfall has greatly improved our ability to predict rainfall patterns over a watershed and offers real advantages for hydrologic flood alert systems.

Chapter 12 is a new chapter on flood control and risk management in the United States and includes a number of new examples from across the country, including discussion of Mississippi River flood control strategies and the surge mitigation response in New Orleans from Katrina. Chapter 13 is also a new chapter for the sixth edition, and details major water resources projects around the United States with detailed case studies from the Colorado River, the Columbia River, major flooding issues in Texas, and a water rights issue between Florida and Georgia.

AUDIENCE AND AVAILABLE RESOURCES

The sixth edition of the text should provide the civil or hydraulic engineering or science student with all the necessary theory to understand principles of hydrology, hydrologic modeling, floodplain hydraulics and analysis, data analysis, and water resources management in the modern digital world. The student or practicing engineer should find the book a useful reference for hydrologic methods, current models, design examples, and extensively documented case studies. In addition, simple calculations and spreadsheet examples are utilized and highlighted in numerous places in the sixth edition, which contains over 80 worked examples, over 220 homework problems, and 13 major case studies.

The Internet offers many sources for access to regional data with minimal cost and effort. Among those, U.S. Geological Survey, National Weather Service, National Resources Conservation Service, U.S. Army Corps of Engineers, and other state and local agencies should be emphasized for students as likely sources of regional hydrologic data. The textbook website (**hydrology.rice.edu)** contains a complete set of PPT slides for classroom instruction, along with datasets, spreadsheets, modeling hints, tutorials, and other resources. Dr. Bedient maintains the website that is available to any instructor and student in the course at no charge. These resources are designed to improve the teaching of a hydrology course at either the undergraduate or graduate level. In addition, an updated **Solutions Manual** is available for instructors. For more details on available resources, see the textbook web site—**hydrology.rice.edu and www.pearsonhighered.com/engineering-resources**.

ACKNOWLEDGMENTS

The current edition of the textbook was developed over a period of 35 years, beginning in 1982, from original course notes in a class in Hydrology and Watershed Analysis at Rice University. During the many years of interaction with colleagues and students, the book evolved into its present form with emphasis on simple examples, clear explanations, and modern computational methods. The sixth edition includes updated text, homework, and examples in all chapters, and new chapters written by a number of amazing colleagues. I am of course indebted to my co-authors, Dr. Wayne Huber and Dr. Baxter Vieux for their invaluable contributions over the years and the new updates in Chapters 3, 6, and 11. I am also indebted to Dr. Wesley Highfield and Dr. Antonia Sebastian for a newly revised Chapter 10, Dr. Antonia Sebastian and Avi Gori for a newly revised Chapter 12, and Dr. Nick Fang, Dr. Andrew Juan, and Catherine Nikiel for a newly revised Chapter 13. Significant example updates are included in Chapter 7 (Dr. Jacob Torres) and Chapter 8 (Dr. Phil DeBlanc). We also thank Dr. Jeri Stedinger of Cornell University for his highly informed help in updating the Bulletin 17B flood frequency analysis procedures described in Chapter 3.

The City of Austin Watershed Protection Department led and funded the project that was used as the SWMM5 Case Study in Chapter 6, Section 8. Geosyntec Consultants was the prime contractor and lead modeler, with assistance from Chan and Partners Engineering, Heather Venhaus, Linda Pechacek, ACR LLC, and Dr. Michael Barrett. Key staff at the City of Austin included Mike Kelly, Leila Gosselink, and Roger Glick.

We are particularly indebted to the following individuals for their careful review of the draft manuscript and for numerous suggestions and comments: Holly Stark, Senior Editor at Pearson, was instrumental in guiding the significant changes for this sixth edition; the authors thank all the professionals at Pearson for their efforts on our behalf, especially Scott Disanno, Carole Snyder, and Preethi Sundar.

A successful textbook always represents a team effort, and the support team at Rice University has been excellent in their organization and great attention to detail. Special thanks are due to Megan Goings and Rik Hovinga at Rice University for their technical skills in organizing and reviewing text and figures, permissions, and for providing valuable input to examples and homework problems. We would also like to thank Rice University students Matt Garcia, Alison Archibal, Bob Zhang, and Toby Li who assisted greatly in developing new problems, solving examples, and developing and checking new homework solutions for the sixth edition.

Philip B. Bedient, *Rice University*
Wayne C. Huber, *Oregon State University, Emeritus*
Baxter E. Vieux, *University of Oklahoma*

ABOUT THE AUTHORS

Philip B. Bedient is the Herman Brown Professor of Engineering with the Department of Civil and Environmental Engineering, Rice University, Houston, TX. He received the PhD degree in environmental engineering sciences from the University of Florida in 1975. He is a registered professional engineer and teaches and performs research in surface hydrology, modeling, and flood prediction systems, and ground water hydrology. He has directed over 60 research projects over the past 41 years, and has written over 200 journal articles and conference proceedings over that time. He has also written four textbooks in the area of surface water and groundwater hydrology. He received the Shell Distinguished Chair in environmental science (1988–92), the C.V. Theis Award in 2007, and he was elected Fellow of ASCE in 2006.

Dr. Bedient has worked on a variety of hydrologic problems nationwide, including river basin analyses, major floodplain studies, flood warning systems, groundwater contamination models, and hydrologic/GIS models in water resources. He has been actively involved in developing radar-based flood prediction and warning, and recently directed the development of a real-time flood alert system (FAS3 and FAS4) for the Texas Medical Center (TMC) in Houston. He has built real-time flood alert systems for several communities across Texas. He currently directs the Severe Storm Prediction Education and Evacuation from Disasters (SSPEED) Center at Rice University, a five-university research organization with private and public entities that predicts and assesses the impacts of severe storms and floods near the Gulf Coast. This center is devoted to developing real-time flood alert and surge alert systems for the coastal areas around Houston such as the Houston Ship Channel, and also evaluates structural and nonstructural methods for mitigation of severe storms. Dr. Bedient has received research funding from the U.S. EPA, the U.S. Department of Defense, NSF, the State of Texas, the U.S. Army Corps of Engineers, the City of Houston, and the Houston Endowment.

Wayne C. Huber is Professor Emeritus of Civil and Construction Engineering at Oregon State University, Corvallis and Senior Consultant with Geosyntec Consultants, Portland, Oregon. His doctoral work at the Massachusetts Institute of Technology dealt with thermal stratification in reservoirs, for which he received the Lorenz G. Straub Award from the University of Minnesota and the Hilgard Hydraulic Prize from the American Society of Civil Engineers (ASCE). Additional awards include the ASCE Environmental and Water Resources Council Julian Hinds Award. He is a member of several technical societies and has served several administrative functions within the ASCE, including service as Associate Editor of the *Journal of Environmental Engineering* since 2007. He is the author of over 120 reports and technical papers, is a registered professional engineer, and has served as a consultant on numerous studies done by public agencies and

private engineering firms. He has served on several review committees of the National Academy of Sciences, including serving as chair of the Committee on Independent Scientific Review of Everglades Restoration Progress.

Beginning at the University of Florida and continuing at Oregon State University, Dr. Huber's research has included studies of urban hydrology, stormwater management, nonpoint source runoff, river basin hydrology, lake eutrophication, rainfall statistics, and hydrologic and water quality modeling. He is one of the original authors of the EPA Storm Water Management Model and helped to maintain and improve the model following its 1971 introduction. Dr. Huber is an internationally recognized authority on runoff quantity and quality processes in urban areas.

Baxter E. Vieux is Professor Emeritus in the School of Civil Engineering and Environmental Science, University of Oklahoma, Norman. He taught courses in hydrology, environmental modeling, GIS applications, water resources, and water quality management after joining OU in 1990, until 2013. Prior to his academic career, he spent 10 years with the USDA Natural Resources Conservation Service (formerly SCS) in Kansas and Michigan, with his highest position as Assistant State Engineer and Acting State Engineer. He is a registered professional engineer in several states and is co-principal and founder of Vieux & Associates, Inc., an engineering technology company with clients in radar-based hydrology. Dr. Vieux is the innovator and architect of the first commercially available physics-based distributed hydrologic model, V*flo*®, which was designed from the outset to use high-resolution maps of terrestrial parameters and radar rainfall. He has authored over 110 publications in hydrology including *Distributed Hydrologic Modeling Using GIS,* 3rd ed., Springer Publishers, Norwell, Massachusetts, Water Science Technology Series, vol. 74. Dr. Vieux has developed and deployed radar-rainfall monitoring and runoff modeling technology for operational hydrologic forecasting services in the United States and internationally.

Chapter 1
Hydrologic Principles

Yellowstone River and Canyon.

Brays Bayou uniform open channel flow.

1.1 INTRODUCTION TO HYDROLOGY

Hydrology is a multidisciplinary subject that deals with the occurrence, circulation, storage, and distribution of surface and ground water on the earth. The domain of hydrology includes the physical, chemical, and biological reactions of water in natural and man-made environments. Because of the complex nature of the hydrologic cycle and its relation to weather inputs and climatic patterns, soil types, topography, geomorphology, and other related factors, the boundary between hydrology and other earth sciences (i.e., meteorology, geology, oceanography, and ecology) is not distinct.

The study of hydrology also includes topics from traditional fluid mechanics, hydrodynamics, and water resources engineering (Maidment, 1993; Mays, 2001). In addition, many modern hydrologic problems include considerations of water quality and contaminant transport. Water quality topics, though important, are not included in this text due to space limitations; they have been covered in a number of modern sources on surface water quality (Huber, 1993; Chapra, 1997; Martin and McCutcheon, 1999) and ground water hydrology and contamination (Bedient et al., 1999; Fetter, 1999; Charbeneau, 2000).

The **hydrologic cycle** is a continuous process in which water is evaporated from water surfaces and the oceans, moves inland as moist air masses, and produces precipitation if the correct vertical lifting conditions exist. The precipitation that falls from clouds onto the land surface of the earth is dispersed to the hydrologic cycle via several pathways (Fig. 1–1). A portion of the **precipitation** *P*, or rainfall, is retained on the soil near where it falls and returns to the atmosphere via **evaporation** *E*, the conversion of water to water vapor from a water surface, and **transpiration** *T*, the loss of water vapor through plant tissue and leaves. The combined loss, called **evapotranspiration** *ET*, is a maximum value if the water supply in the soil is adequate at all times. These parameters are further discussed in subsequent sections of this chapter and Section 2.6.

Some water enters the soil system as **infiltration** *F*, which is a function of soil moisture conditions and soil type, and may reenter channels later as interflow or may percolate to recharge the shallow ground water. **Ground water** *G* flows in porous media in the subsurface in either shallow or deeper aquifer systems that can be pumped for water supply to agricultural and municipal water systems (see Chapter 8).

The remaining portion of precipitation becomes overland flow or **direct runoff** *R*, which flows generally in a down-gradient direction to accumulate in local streams that then flow to rivers. Hydrologic analysis to determine runoff response from a watershed area is covered in Chapter 2. Evaporation and infiltration are both complex losses from input rainfall and are difficult to measure or compute from theoretical methods, covered in detail in Sections 2.6, 2.7, and 2.8.

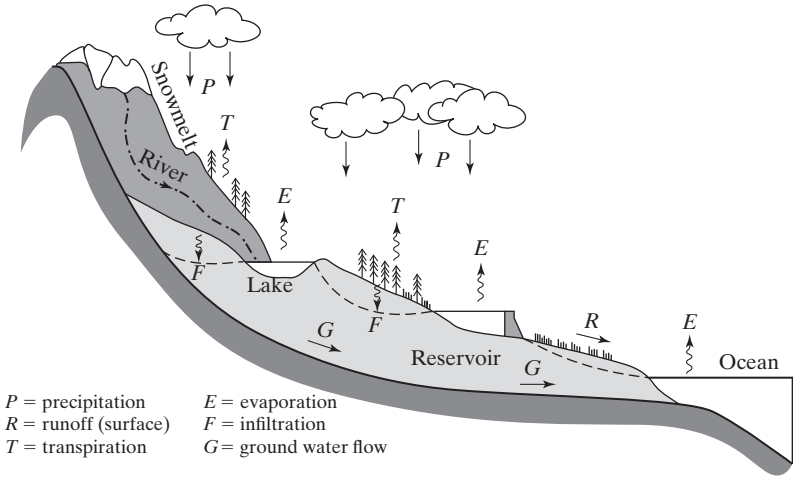

Figure 1–1(a)
The hydrologic cycle discharges surface water and groundwater from the higher elevation to the lower elevation.

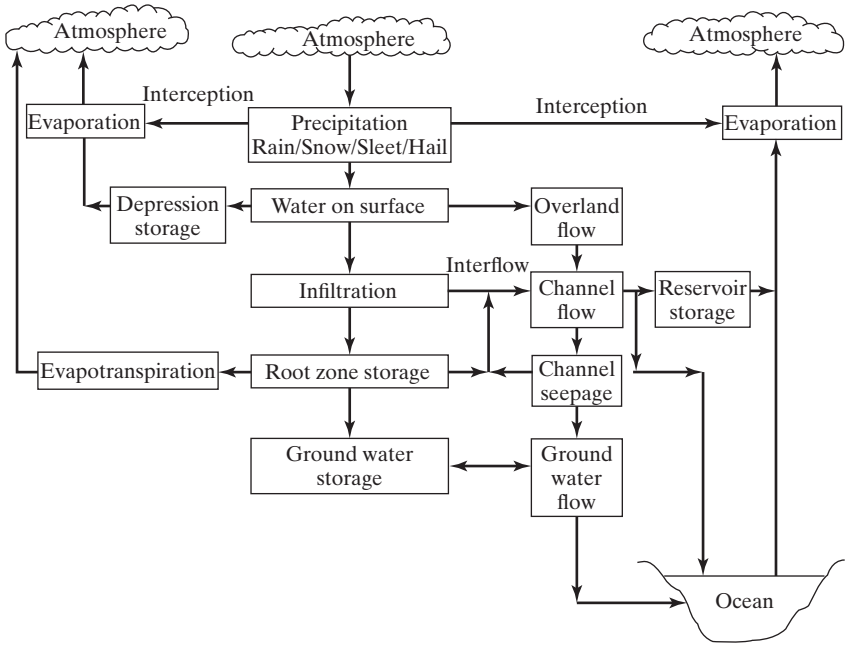

Figure 1–1(b)
Flow chart of the components of the hydrologic cycle.

Surface and ground waters flow from higher elevations toward lower elevations and may eventually discharge into the ocean, especially after large rainfall events [Fig. 1–1(a)]. However, large quantities of surface water and portions of ground water return to the atmosphere by evaporation or *ET*, thus completing the natural hydrologic cycle [Fig. 1–1(b)]. Precipitation from the atmosphere is a major force that drives the hydrologic cycle, and understanding major weather parameters and systems is important for the prediction of precipitation events (see Section 1.2).

Ancient History

Biswas (1972), in a concise treatment of the history of hydrology, describes the early water management practices of the Sumerians and Egyptians in the Middle East and the Chinese along the banks of the Huang He (Yellow River). Archeological evidence exists for hydraulic structures that were built for irrigation and other water control activities. A dam was built across the Nile about 4000 B.C., and later a canal for fresh water was constructed between Cairo and Suez.

The Greek philosophers were the first serious students of hydrology, with Aristotle proposing the conversion of moist air into water deep inside mountains as the source of springs and streams. Homer suggested the idea

Figure 1–2
Roman aqueduct in Segovia, Spain.

of an underground sea as the source of all surface waters. The Romans constructed numerous aqueducts to serve large cities as well as small towns and industrial sites. The Romans had the largest collection with water being supplied by 11 aqueducts constructed over a period of about 500 years. Figure 1–2 shows one of the famous aqueducts built in Europe during that early period. They served potable water and supplied the numerous baths and fountains in the city, as well as finally being emptied into the sewers, where the once-used gray water performed their last function in removing wastes. The construction of the Roman aqueducts is considered one of the most important engineering feats in history.

Streamflow measurement techniques were first attempted in the water systems of Rome (A.D. 97) based on the cross-sectional area of flow. It remained for Leonardo da Vinci to discover the proper relationship between area, velocity, and flow rate during the Italian Renaissance. The first recorded measurement of rainfall and surface flow was made in the seventeenth century by Perrault. He compared measured rainfall to the estimated flow of the Seine River to show the two were related. Perrault's findings were published in 1694. Halley, the English astronomer (1656–1742), used a small pan to estimate evaporation from the Mediterranean Sea and concluded that it was enough to account for tributary flows. Mariotte gaged the velocity of flow in the Seine River in Paris. These early beginnings of the science of hydrology provided the foundation for numerous advances in the eighteenth century, including Bernoulli's theorem, the Pitot tube for measuring velocity, and the Chezy (1769) formula, which form the basis for modern hydraulics and fluid measurement.

During the nineteenth century, significant advances in ground water hydrology and hydraulics occurred. Darcy's law for flow in porous media was a major advance, as well as the Dupuit–Thiem well flow formula (Chapter 8). In addition, the Hagen–Poiseuille capillary flow equation was developed

to describe flow in small channels. The Darcy–Weisbach equation for pipe flow was also developed during this same period in the 1850s. In surface water hydrology, many flow formulas and measuring instruments were developed that allowed for the beginning of systematic stream gaging. In 1867, discharge measurements were organized on the Rhine River at Basel and quickly expanded throughout Europe.

The U.S. Geological Survey set up the first systematic program of flow measurement in the United States on the Mississippi in 1888. During this same period, the United States founded a number of hydrologic agencies, including the U.S. Army Corps of Engineers (1802), the U.S. Geological Survey (USGS, 1879), the Weather Bureau (1891), and the Mississippi River Commission (1893). The Price current meter was invented in 1885, and Manning's formula was introduced in 1889 (Manning, 1889). The Weather Bureau is now called the National Weather Service (NWS) and is one of six organizations underneath the National Oceanic and Atmospheric Administration (NOAA). NOAA is the agency responsible for weather data collection and severe-storm, river, and hurricane forecasting for the United States, and many of its websites are listed throughout the textbook. The USGS gaging network for rainfall, streamflow, and water quality is one of the most extensive in the world (see Appendix E).

Early History (1930s–1950s)

The period from 1930 to 1950, which Chow (1964) called the Period of Rationalization, produced a significant step forward for the field of hydrology, as government agencies began to develop their own programs of hydrologic research. Sherman's unit hydrograph (1932) (see Chapter 2), Horton's infiltration theory (1933), and Theis's nonequilibrium equation (1935) in well hydraulics (Chapter 8) advanced the state of hydrology in very significant ways. Gumbel (1958) proposed the use of extreme-value distributions for frequency analysis of hydrologic data, thus forming the basis for modern statistical hydrology (Chapter 3). In this period, the U.S. Army Corps of Engineers (ACOE), the NWS within NOAA, the U.S. Department of Agriculture (USDA), and the USGS made significant contributions in hydrologic theory and the development of a national network of gages for precipitation, evaporation, and streamflow measurements. The NWS is still largely responsible for rainfall measurements, reporting and forecasting of severe storms, and other related hydrologic investigations.

The U.S. ACOE and the USDA Soil Conservation Service (now called the Natural Resources Conservation Service [NRCS]) made significant contributions to the field of hydrology in relation to flood control, reservoir development, irrigation, and soil conservation during this period. More recently, the USGS has taken significant strides to set up a national network of stream gages and rainfall gages for both quantity and quality data. Their water supply publications and special investigations have done much to advance the field of hydrology by presenting the analysis of complex hydrologic data

to develop relationships and explain hydrologic processes. The NWS and USGS both support numerous websites for the dissemination of watershed information and precipitation and streamflow data from thousands of gages around the country. Many of these sites are listed in Appendix E and on the textbook website (hydrology.rice.edu).

The government agencies in the United States have long performed vital research themselves, providing funding for private and university research in the hydrologic area. Many of the water resources studies and large dam, reservoir, and flood control projects in the 1930s and 1940s were a direct result of advances in the fields of fluid mechanics, hydrologic systems, statistical hydrology, evaporation analysis, flood routing, and operations research. Many of the advances from that era continue to this day as the methods to predict runoff, infiltration, and evaporation have not changed much in over 50 years. Major contributions from Horton (1933, 1940, 1941) and from Penman (1948) in understanding hydrologic losses were related to the water and irrigation needs of the agricultural sector in the United States following the devastation of the dust bowl era of the 1930s.

Major water resources projects built during the 1930s were a direct result of major floods on the Mississippi River and the economic depression across the nation. The building of the massive Hoover Dam on the Colorado River for flood and sediment control and water supply in the early 1930s provided employment for thousands and was the largest construction project ever conceived to that point (see Chapters 12 and 13).

Modern History

In the 1950s and 1960s, the tremendous increase of urbanization following World War II in the United States and Europe led to better methods for predicting peak flows from floods, for understanding impacts from urban expansion, and for addressing variations in storage in water supply reservoirs. Major expansion of cities and water systems within the United States during the 1950s led to a need for better understanding of floods and droughts, especially in urban areas. Water resource studies became an everyday occurrence in many rapidly developing areas of the United States, tied to the expansion of population centers in the southern, southwestern, and western states. Hydrologic analyses presented in detail in Chapters 2 through 9 in the text were a major component of many of these studies.

During the 1970s and early 1980s, the evaluation and delineation of floodplain boundaries became a major function of hydrologists, as required by the Federal Emergency Management Agency (FEMA) and local flood control or drainage districts. In order for communities to be eligible for flood insurance administered by FEMA, they are required to delineate floodplain boundaries using hydrologic analysis and models. Floodplain analysis is covered in detail in Chapters 5, 7, 9, and 12. This function has taken on a vital role in many urban areas, as damages from severe floods and hurricanes continue to plague the United States, especially in coastal and low-lying areas.

The period from 2004 to 2016 accounted for numerous hurricanes that caused massive damages and deaths in several areas, especially along the coastlines of Texas, Louisiana, Mississippi, Alabama, and Florida. The massive Mississippi flood of 1993 wreaked havoc within the central United States, and was repeated in 2011 with major devastation to states from Illinois south to Louisiana (Chapter 12). Major floods again devastated parts of Texas and Louisiana in both 2015 and 2016 (Chapter 13).

In recent years, the traditional approaches to flood control have been reassessed. A study titled "Higher Ground" from the National Wildlife Federation (1998) found a number of communities with large numbers of repetitive flood losses, such as New Orleans and Houston. Since the great midwestern flood of 1993, there has been a significant shift in national flood policy away from using only structural solutions, such as levee and channel construction. Flood damage from Tropical Storm Allison in Houston in 2001 was a major wake-up call for better protection and warning systems in critical urban areas. The massive devastation from Hurricane Katrina in New Orleans in August 2005 and Hurricane Ike in 2008 in Houston-Galveston will provide long-lasting incentive to improve our ability to warn for and recover from such severe storms. Modern methods for structural flood control, as well as nonstructural approaches, better management of flood-prone areas, and voluntary property buyouts, must be considered in any overall flood management plan (Chapter 12). Chapter 13 explores several major water resources projects across the United States in terms of engineering significance as well as associated environmental and policy impacts on the nation.

Computer Advances

The introduction of the digital computer into hydrology during the 1960s and 1970s allowed complex water problems to be simulated as complete systems for the first time. Large computer models can now be used to match historical data and help answer difficult hydrologic questions (Singh and Frevert, 2006). The development of these tools over the past few decades has helped direct the collection of the hydrologic data to calibrate, or "match," the models against observation. In the process, the understanding of the hydrologic system has been greatly advanced. Hydrologic computer models developed in the 1970s have been applied to areas previously unstudied or only empirically defined. For example, urban stormwater, floodplain and watershed hydrology, drainage design, reservoir design and operation, flood frequency analysis, and large-river basin management have all benefited from the application of computer models.

Hydrologic simulation models applied to watershed analysis are described in detail in Chapters 5 and 6. Single-event models such as HEC-HMS are used to simulate or calculate the resulting storm hydrograph (discharge vs. time) from a well-defined watershed area for a given pattern of rainfall intensity. Continuous models such as the Hydrological Simulation Program—Fortran (HSPF) and the Storm Water Management Model (SWMM) can account for soil moisture storage, evapotranspiration, and

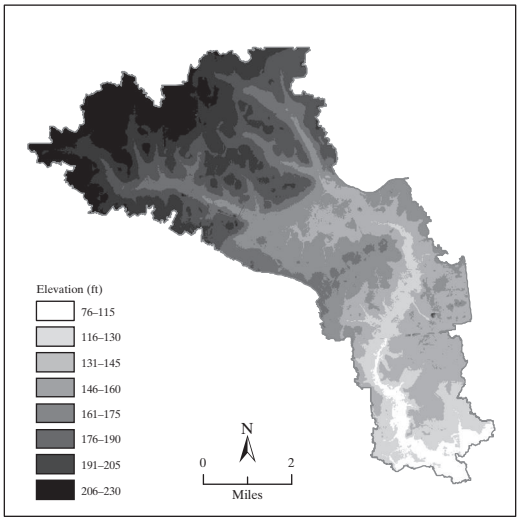

Figure 1–3
GIS map of typical watershed.

antecedent rainfall over long time periods. Statistical models can be used to generate a time series of rainfall or streamflow data, which can then be analyzed with flood frequency methods.

Newer distributed hydrologic models (i.e., VFLO and the MIKE series of models) can handle input, output, and data manipulation at the watershed level (see Chapters 5, 10, 11, and 12). Unquestionably new digital approaches combined with distributed terrain modeling have revolutionized hydrology in recent years, just as the original wave of hydrologic and hydraulic models did in the decade of the 1970s. Also faster computers and available datasets have been instrumental in advancing the field.

The data revolution in hydrology and geographical information systems (GIS) has made available newer and more accurate datasets on topography, slope, rainfall, soils, land use, and channel characteristics for many areas. Moreover, most hydrological and meteorological data may be retrieved online from agencies such as the USGS and NWS, and various county and municipal sources. These datasets, combined with existing simulation models in hydrology, if applied correctly, provide the most accurate approach to understanding complex water resources systems, and a new era in the science of hydrology has begun this decade. New design and operating policies are being advanced and implemented that could not have been realized or tested before without the aid of sophisticated computer models linked with digital data (Fig. 1–3).

1.2 WEATHER SYSTEMS

The atmosphere is the major hydrologic link between oceans and continents on the planet, facilitating the cycle of water movement on earth. The hydrologic cycle is shaped by the conditions of the atmosphere, with precipitation as the main input to the cycle. Water vapor content is both a major catalyst and a balancing factor of atmospheric processes that create the weather

in the lower atmosphere. The following section reviews major elements of atmospheric processes that directly impact the hydrologic cycle. More details on atmospheric processes can be found in modern meteorology and hydrology textbooks (Anthes, 1997; Ahrens, 2000; Dingman, 2002).

Atmospheric Parameters

Pressure is defined as the force per unit area exerted on a surface, and **atmospheric pressure** measures the weight of the air per unit area. Average air pressure at sea level is approximately 1 atmosphere, or 1013 millibars (mb) or 14.7 lb/in.^{2} or 760 mm-Hg or 29.97 in.-Hg. Note that 1 mb $= 10^2$ pascals (Pa), where 1 Pa $= 1$ N/m^2. As elevation increases and the density of air molecules decreases, atmospheric pressure also decreases. The horizontal and vertical pressure variations that occur due to low- and high-pressure systems are responsible for wind, and help drive much of our weather. Absolute temperature (T), pressure (P), and density (ρ) are related through the ideal gas law, $P = \rho RT$, where R is the gas constant for the gas in question (see Eq. 1–1). At constant density, temperature is directly proportional to pressure; thus, with an increase in temperature comes an increase in pressure. Air pressure is proportional to density, so that in the atmosphere a decrease in temperature causes an increase in the density of the air molecules. Cold air masses are generally associated with the higher atmospheric pressure.

Humidity is a measure of the amount of water vapor in the atmosphere and can be expressed in several ways. Specific humidity is the mass of water vapor in a unit mass of moist air. The **relative humidity** is a ratio of the air's actual water vapor content compared to the amount of water vapor at saturation for that temperature. The partial pressure of water vapor is the contribution made by water to the total atmospheric pressure. When a volume reaches its maximum capacity for water vapor, the volume is said to be saturated and can accept no more vapor. This vapor pressure is known as **saturation vapor pressure**. Vapor pressure is dependent on temperature, and as air is lifted and cools, its relative humidity increases until saturation, and then condensation of water vapor to liquid water can occur. The temperature to which a sample of air must be cooled to reach saturation is defined as the **dew point temperature**. These concepts are described in more detail later in this section.

Water vapor has the ability, unique among gases, to change from one state of matter to another (solid, liquid, or gas) at the temperatures and pressures that typically exist on earth. A change in phase (e.g., from liquid to vapor) requires that heat be released or absorbed. The processes of converting solid ice to liquid water, called melting, and water to vapor, called evaporation, both require significant heat exchange. It takes approximately 600 cal to convert 1 g of water to water vapor. When such changes take place, the heat is absorbed and no temperature change takes place. The heat used in this process is latent heat. Condensation is the process in which water vapor changes into a liquid state. For this to occur, energy must be released

in an amount equivalent to what was absorbed during evaporation. This latent heat often becomes the source of energy for severe thunderstorms, tornadoes, and hurricanes.

The Atmosphere and Clouds

Atmospheric weather systems are fueled by solar input and characterized by air masses in motion, circulating winds, cloud generation, and changes in temperature and pressure. Lifting mechanisms are required for moist air masses to cool and approach saturation conditions. As a result of the interaction of rising air masses with atmospheric moisture, the presence of small atmospheric nuclei, and droplet growth, precipitation in the form of rain, snow, or hail can result. The exact mechanisms that lead to precipitation are sometimes quite complex and difficult to predict for specific areas. But precipitation remains as the main input to the hydrologic cycle, and the hydrologist needs a general understanding of the mechanisms that cause its formation.

Horizontal variations in atmospheric pressure cause air to move from higher pressure toward lower pressure, resulting in the generation of wind. Vertical displacement causes air to move as well, but at a far slower rate than horizontal winds. The vertical movement and lifting of air results in the formation of clouds. Clouds are familiar to all of us, and represent collections of small droplets of water or tiny crystals of ice. The names of the basic clouds have the following roots:

cirrus, feathery or fibrous clouds

stratus, layered clouds

cumulus, towering, puffy clouds

alto, middle-level clouds

cumulonimbus, rain clouds

The second aspect of cloud classification is by height. Anthes (1997) presents a detailed coverage of cloud types for the interested student. One type of high cloud of importance in hydrology is the **cumulonimbus**, one often found in heavy thunderstorms that produce massive rainfall. Cirrus clouds are very high collections of ice crystals and often indicate the approach of a cold front and that weather is about to change. While clouds result when air rises and cools, surface fog results from cooling near the surface or from the addition of enough water vapor to cause saturation. Fog is essentially a low cloud with a base that is very near the ground, often reducing the visibility in the area within or around it. Marine fog is common along the California and upper Atlantic coasts in the United States.

General Circulation

The general circulation of wind across the earth is caused by the uneven heating of earth's surface through solar input, and by the earth's rotation. At the equator, solar radiation input and temperature are greatest because of the

shape and tilt of the globe relative to the sun. Three latitudinal circulation cells transport heat from the equator to the poles (Fig. 1–4). As warm air travels northward in the middle latitudinal cell on a spinning earth, it tends to shift to the right (toward the east) in the northern hemisphere due to the Coriolis force, thus causing the occurrence of winds called **westerlies**. These winds tend to drive the direction of major weather systems from west to east across major portions of the continental United States.

Between 30 degrees north latitude and the equator, the flow is generally toward the south and is altered to create the trade winds (**easterlies**) by the Coriolis force in the northern hemisphere. The trade winds allowed explorers from Europe to sail across the ocean to the New World. The Coriolis force causes the flow along latitude circles (east/west) to be 10 times greater than the flow along the meridians (north/south). Around the 30 degrees north and south latitudes, descending air creates a region of minimal winds and little cloudiness that is known as the horse latitudes. Near the equator is another region of light and variable winds called the doldrums, or the intertropical convergence zone. This is the area of maximum solar heating, where surface air rises and flows toward both poles.

Jet streams, first observed in 1946, are narrow bands of high-speed winds that circle each hemisphere like great rivers, at elevations extending from 2.5 or 3 miles to above the tropopause. The polar and subtropical jets

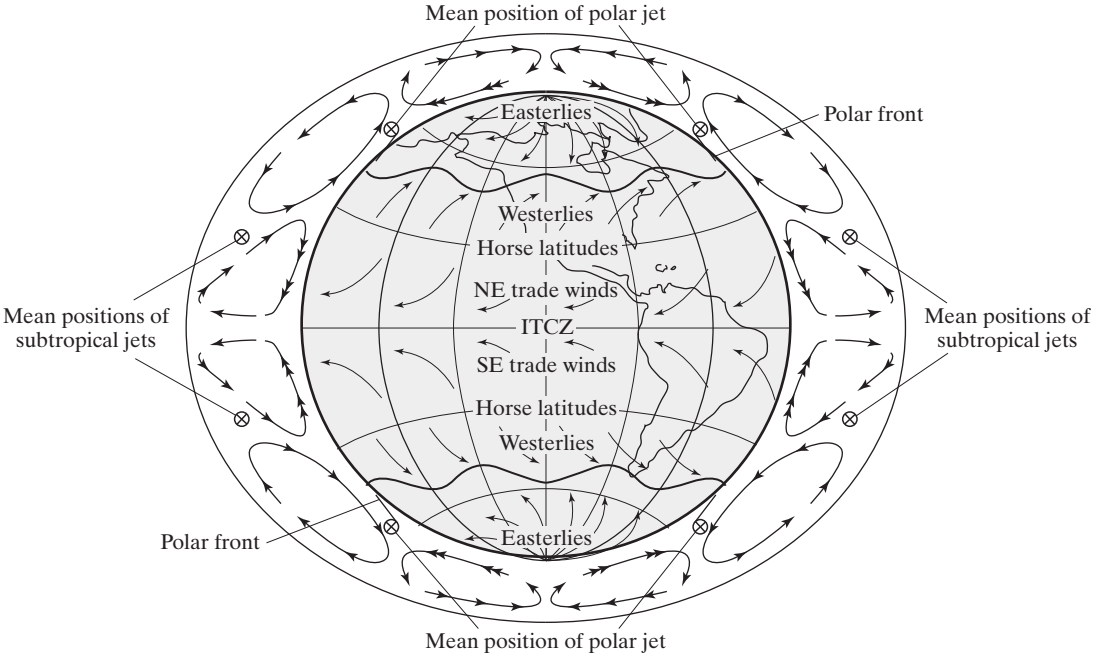

Figure 1–4
General circulation of currents and wind patterns across the earth.

are associated with the polar front near 45 degrees latitude and 30 degrees latitude, respectively. The jet streams are highly variable and can flow at speeds as high as 100 mph faster than the air on either side of them. Jet streams have a major impact as the driving force for weather systems across the United States, especially in the winter season.

Air Masses and Fronts

Air masses are large bodies of air with fairly consistent temperature and humidity gradients in the horizontal direction at a given altitude. Air masses dominate our weather and are classified in two ways: the source from which they were generated, land (continental) or water (maritime), and the latitude of generation (polar or tropical). The four combinations are designated cP, cT, mP, and mT.

Each of these types of air masses is present in the United States. The continental polar air mass emanates from Canada and passes over the northern United States, often dropping significant amounts of rain and snow on areas downwind of the Great Lakes. The maritime polar air mass also comes southward from the Atlantic coast of Canada and affects the New England states. Another maritime polar air mass comes from the Pacific and hits the extreme northwestern states. The maritime tropical air masses come from the Pacific, the Gulf of Mexico, and the Atlantic. The entire southern United States is affected by these air masses. The only time continental tropical air masses form is during the summer, and they originate in Texas and affect the states bordering to the north.

The boundary between one air mass and another is called a frontal zone, or **front**. When two air masses meet, the front will slope diagonally, as the colder, denser air mass pushes under the warmer air mass. Between the two fronts, a transition zone occurs, usually 30 to 60 miles wide. Whether the masses are traveling against each other or in the same direction, the warmer air mass will be forced upward and cooled by expansion. Since cooling a parcel of air lowers its saturation vapor pressure, this may cause condensation and the development of precipitation often associated with frontal systems (Fig. 1–5). The NWS website provides an amazing amount of weather information and satellite data all on one place (http://www.nws.noaa.gov/).

Development of surface cyclones along fronts occurs when an upper-level disturbance approaches a front. The upper-level patterns of convergence and divergence produce pressure changes at the surface, which then produce low-level circulation (**wave cyclone**). As a wave cyclone develops, low pressure forms at its apex and both the warm and cold currents move in a cyclonic pattern (counterclockwise in the northern hemisphere) around it. To the left of the apex, the cold front is advancing toward the warm air, and the warm front is receding to the right. The warm air between the fronts is known as the warm sector. The entire system generally moves toward the right (eastward), and ahead of the warm front the first sign of the approaching system is high cirrus clouds. As the center of low pressure

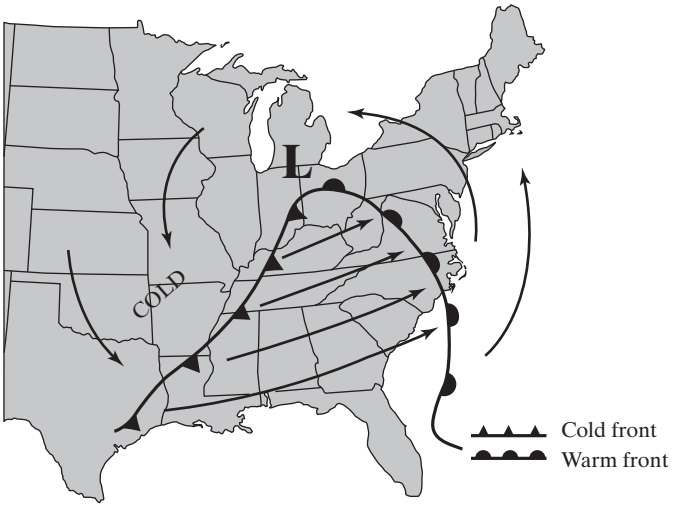

Figure 1–5
Direction of the cold and warm fronts in the eastern United States. The cold fronts come from the North toward the Gulf and the warm fronts start from the Gulf to push inland.

approaches, the pressure falls and the wind increases and changes its direction to counterclockwise. The temperature begins to decrease as the frontal zone approaches. Within several hundred miles of the surface position of the front, precipitation begins, either rain or snow. Fronts can be fast moving in the winter or can be slowed or stalled due to the presence of other air masses or high-pressure systems in the fall or spring (Anthes, 1997). Warm fronts can also generate rainfalls as they move across an area.

Fronts are a major factor in U.S. weather patterns, especially from September through April in most years. The type of weather accompanying the passage of the cold front depends on the front's sharpness, its speed, and the stability of the air being forced aloft. Often there are towering cumulus clouds and showers along the forward edge of the front. Sometimes, especially in the Midwest during the spring, several **squalls**, or a strong line of storms, precede the front. Tornadoes can form in these storm cells, especially in areas of north Texas, Oklahoma, and Arkansas. But in other cases, nimbostratus clouds and rain extend over a zone of 50 to 60 miles. After the frontal passage, the wind changes sharply and the pressure begins to rise. Within a short distance behind the cold front, the weather clears, the temperature begins to fall, and the visibility greatly improves.

Thunderstorms

Thunderstorm activity is characterized by cumulonimbus clouds that can produce heavy rainfall, thunder, lightning, and occasionally hail. Thunderstorms are the result of strong vertical movements in the atmosphere and

usually occur in the spring or summer in the United States. They require warm, moist air, which when lifted will release enough latent heat to provide the buoyancy needed to maintain its upward motion. Accordingly, they generally occur in warm air masses that have become unstable either through extreme low-pressure systems, surface heating, or forced ascent over mountains. The geographic pattern of thunderstorm occurrence in the United States is a result of both an area's distance from source air masses and its topography. Florida and the Gulf Coast are affected most frequently, sometimes as often as 100 times in a year.

Thunderstorms develop in three characteristic stages. The first is the cumulus stage, when moist air rises and cools and condenses into a cumulus cloud. The cumulonimbus cloud then continues to grow taller as the rising air condenses at successively higher levels [Fig. 1–6(a)]. The diameter of the storm cell grows in width from about 1 mile to 6 to 9 miles and vertically to 5 or 6 miles. The rising air is no longer able to retain water droplets and rain begins to fall.

The rain marks the beginning of the second stage of the thunderstorm, the mature stage. During the mature stage, the large water particles or hail in the clouds begin to fall because they have become too large to be supported by the updraft. As this happens, drier air around the cloud is being drawn into it, in a process known as entrainment. This drying of the air results in the evaporation of some rain drops, which cools the air. The air is now colder and heavier than the air around it and, while the upper part of the cloud still has a strong updraft, a lower part of the storm cloud begins to descend as a downdraft. This downdraft eventually reaches the ground and spreads away from the thunderstorm, causing the cool gusts of wind that usually foreshadow the arrival of a thunderstorm. Meanwhile, the upper part of the cloud reaches a stable part of the atmosphere, and high-altitude winds may create a typical anvil shape [Fig. 1–6(b)]. The cloud reaches its greatest

Figure 1–6(a)
The cumulonimbus cloud that signals that a storm is approaching.

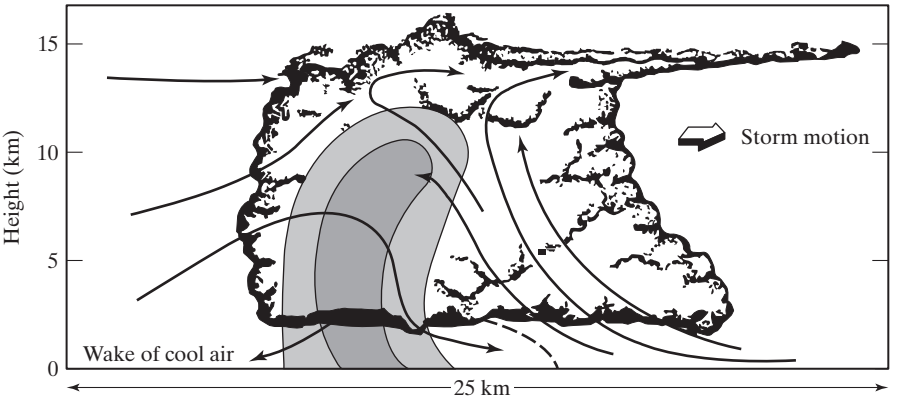

Figure 1–6(b)
Typical thunderstorm cloud evolution. The typical anvil-shaped clouds that are present during a thunderstorm are caused by the movement of cold air and warm air. As the cold air moves downward and the warm air moves upward, the warm air above spreads out in order to cool, resulting in the above shape, very much like an anvil.

vertical development in this stage, extending upward over 7.5 mi (40,000 ft, 12 km). Lightning, turbulence, heavy rains, and, if present, hail are all found at this time. The second stage is the most intense period of the thunderstorm.

When the downdraft has spread over the entire storm cell and the updraft has been cut off, the storm begins its final stage, the dissipating stage. The rate of precipitation diminishes and so the downdrafts are also gradually subdued. The final flashes of lightning fade away and the cloud begins to dissolve or perhaps persist a while longer in a stratified form [see Fig. 1–6(b)]. Intense thunderstorms are of great interest, since they can produce significant amounts of rainfall in a short time period. Chapter 11 discusses modern radar methods for the detection of severe storms and for the measurement of rainfall intensities associated with severe storms.

Hurricanes

Tropical cyclones or **hurricanes** are intense cyclonic storms that form over the tropical oceans, between 5 and 20 degrees latitude. With extreme amounts of rainfall and winds that can exceed 186 mph (300 km/hr), tropical cyclones are the most destructive storms on earth. The local name for this storm varies throughout the world: typhoon in Eastern Asia, cyclone in India, and baguio in the China Sea. The North American term, used in this discussion, is hurricane. By international agreement, a storm is a hurricane if it has wind speeds of at least 74 mph (119 km/hr) and a rotary circulation. When its wind speeds are between 39 mph (63 km/hr) and 73 mph (119 km/hr), it is a tropical storm. Tropical disturbances with winds that do not exceed 39 mph (61 km/hr) are tropical depressions. All tropical storms and hurricanes are given proper names in alphabetical order, starting at the beginning

of the alphabet when the storm season begins on June 1 and starting over during the next season. Hurricanes are classified according to a scale based on central pressure, storm surge height, and wind speed. The Saffir–Simpson scale has five categories, ranging from category 1, a hurricane of minimal damage, to category 5, a hurricane of catastrophic proportions (see Fig. 1–7).

The warm, moisture-laden air of the tropical oceans possesses an enormous capacity for heat energy, and most of the energy required to create and sustain a hurricane comes from what is released through condensation from vapor to water. Hurricanes develop most often during the late summer when the oceans are warm (26°C or higher) and are thus able to provide the necessary heat and moisture to the air. The hurricane season in the West Indies extends from June 1 to November 1, but 84% of the hurricanes and tropical cyclones below hurricane intensity reported from 1887 to 1958 in the North Atlantic occurred during August, September, and October. There is considerable variability in the number of hurricanes in the Atlantic annually. In the 40-year period from 1950 to 1990, the number of hurricanes in the Atlantic varied from 3 to 12 per year.

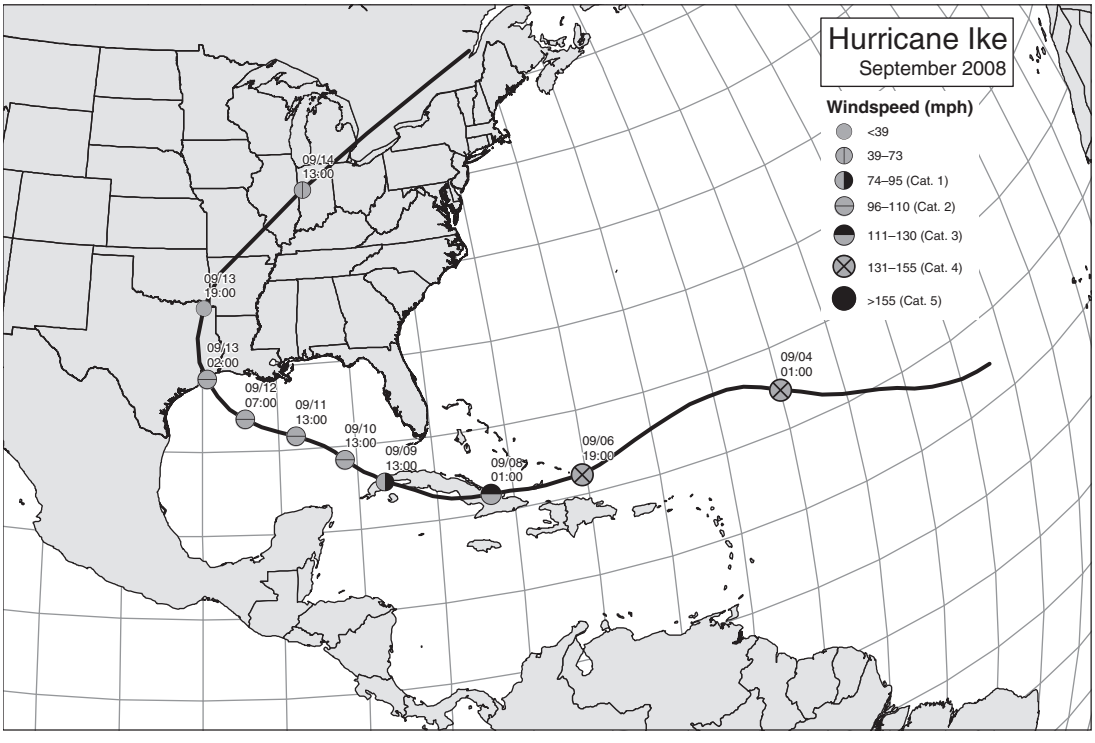

Figure 1–7
Hurricane Ike's track. The hurricane started in the Atlantic and made its way into the Gulf. What started out as a Category 4 storm in the Atlantic became a Category 3 as it hit Cuba and finally weakened to a Category 2 storm as it made landfall in Texas.

The decades of the 1990s and 2000s have seen especially high hurricane activity in the North Atlantic basin, including both hurricane frequency and intensity. As indicated below, 2004–2008 were very active hurricane years for the coastal United States. Figure 1–7 shows the devastating track of Hurricane Ike that damaged the Houston-Galveston coastline in September, 2008. Statistics have shown that the number of tropical storms correlates with several climatological anomalies on a global scale, including rainfall in West Africa in the prior year, the direction of the winds in the stratosphere, and the **El Niño-Southern Oscillation (ENSO)** phenomenon, characterized by a warm phase associated with high sea surface temperatures off the coast of Peru, low atmospheric pressure over the eastern Pacific, high pressure in the western Pacific, and strong winds aloft over the tropical Atlantic (creating high vertical wind shear and unfavorable conditions for hurricane development). A cold phase (**La Niña**) has low sea surface temperatures in the eastern Pacific and the opposite pressure and wind anomalies. Meteorology textbooks and websites usually provide more details on the occurrence and characteristics of hurricanes (Anthes, 1997; Ahrens, 2000; Dingman, 2002). More details on recent hurricanes and their damaging impacts can be found in Chapter 12.

Moisture Relationships

Atmospheric moisture is a necessary source for precipitation and is generally provided from evaporation and transpiration. Precipitation across the United States is largely due to proximity of evaporation from oceans and the Gulf of Mexico and to subsequent transport over the continent by the atmospheric circulation system. Common measures of atmospheric moisture, or humidity, include vapor pressure, specific humidity, mixing ratio, relative humidity, and dew point temperature. (Most of these terms were defined earlier in the chapter.) Under moist conditions, water vapor can be assumed to obey the ideal gas law, which allows derivation of simple relations between pressure, density, and temperature.

The partial pressure is the pressure that would be exerted on the surface of a container by a particular gas in a mixture. The partial pressure exerted by water vapor is called **vapor pressure** and can be derived from Dalton's law and the ideal gas law as

$$e = \frac{\rho_w RT}{0.622}, \tag{1–1}$$

where

e = vapor pressure (mb),
ρ_w = vapor density or absolute humidity (g/cm^3),
R = dry air gas constant = 2.87×10^3 mb cm^3/g°K,
T = absolute temperature (°K).

The factor 0.622 arises from the ratio of the molecular weight of water (18) to that of air (29). Near the earth's surface, the water vapor pressure is 1% to 2% of the total atmospheric pressure, where average atmospheric pressure is 1013.2 mb (1 mb $= 10^2$ pascals (Pa)). **Saturation vapor pressure** is the partial pressure of water vapor when the air is completely saturated (no further evaporation occurs) and is a function of temperature.

Relative humidity (RH) is approximately the ratio of water vapor pressure to that which would prevail under saturated conditions at the same temperature. It can also be stated as $RH = 100\, e/e_s$. Thus, 50% relative humidity means that the atmosphere contains 50% of the maximum moisture it could hold under saturated conditions at that temperature. Typical relative humidity averages (high and low percentages) for eight major American cities are as follows: Houston (89, 67), Seattle (84, 62), Chicago (80, 64), New York City (72, 56), Miami (83, 61), Denver (67, 40), Albuquerque (58, 29), and Las Vegas (40, 21).

Specific humidity is the mass of water vapor contained in a unit mass of moist air (g/g) and is equal to ρ_w/ρ_m, where ρ_w is the vapor density and ρ_m is the density of moist air. Using Dalton's law and assuming that the atmosphere is composed of only air and water vapor, we have

$$\rho_m = \frac{(P - e) + 0.622e}{RT} = \frac{P}{RT}(1 - 0.378e/P). \tag{1–2}$$

Equation (1–2) shows that moist air is actually lighter than dry air for the same pressure and temperature. Thus,

$$q = \frac{\rho_w}{\rho_m} = \frac{0.622e}{P - 0.378e}, \tag{1–3}$$

where

q = specific humidity (g/g),
e = vapor pressure (mb),
P = total atmospheric pressure (mb),
ρ_m = density of mixture of dry air and moist air (g/cm^3).

Finally, the **dew point temperature** T_d is the value at which an air mass just becomes saturated ($e = e_s$) when cooled at constant pressure and moisture content. An approximate relationship for saturation vapor pressure over water e_s as a function of temperature T is

$$e_s = 2.7489 \times 10^8 \exp\left(-\frac{4278.6}{T + 242.79}\right), \tag{1–4}$$

where e_s is in mb and T is in °C. The relationship is accurate to within 0.5% of tabulated values (List, 1966) over a range of temperatures from 0°C to 40°C. Homework problems for Chapter 1 and the following Example 1.1 explore the use of Eq. (1–4) in more detail to compute relative humidity. More details on their application and use can be found in standard textbooks (Wallace and Hobbs, 1977; Ahrens, 2000; Dingman, 2002).

EXAMPLE 1–1

At the airport, weather specialist measured the air pressure to be 124.3 kPa, the air temperature was 28°C, and the dew point temperature was 20°C. Calculate the corresponding vapor pressure, relative humidity, and specific humidity. First compute e and e_s.

SOLUTION

Air pressure = 124.3 kPa = 1243 mb

Air temp = 28°C

T_d = 20°C

*Hint: 100 Pa = 1 mb

Vapor Pressure

$$e = 2.749 \times 10^8 \exp\left(\frac{-4278.6}{T_d + 242.79}\right), \text{ plug in 20°C for } T \text{ to get 23.34 mb}$$

$$e_s = 2.7489 \times 10^8 \exp\left(-\frac{4278.6}{T + 242.79}\right), \text{ plug in 28°C for } T \text{ to get 37.56 mb}$$

Relative Humidity

$$H = 100\,{}^{e}\!/_{e_s} = 100 \cdot {}^{23.34}\!/_{37.56} = 100 \cdot 0.62 = 62\%$$

Specific Humidity

$$q = \frac{\rho_w}{\rho_m} = \frac{0.622e}{P - 0.378e}, \text{ plug in 23.34 mb for } e \text{ and 1243 mb for } P \text{ to get 0.0117 kg}$$

water/kg moist air

Atmospheric Stability and Phase Changes

In order for vapor to condense to water to begin the formation of precipitation, a quantity of heat known as latent heat must be removed from the moist air. The **latent heat** of condensation L_c is equal to the latent heat of evaporation L_e, the amount of heat required to convert water to vapor at the same temperature. With T measured in °C,

$$L_e = -L_c = 597.3 - 0.57(T - 0°\text{C}), \tag{1–5}$$

where L_e is in cal/g. The latent heat of melting and freezing are also related:

$$L_m = -L_f = 79.7,$$

where L_m is also in cal/g. Thus, it takes about 7.5 times the energy to evaporate a gram of water compared to melting a gram of ice.

As moist, unsaturated air rises, the relative humidity increases, and at some elevation saturation is reached and relative humidity becomes 100%. Further cooling of the air results in condensation of the moisture at a defined lifting condensation level (LCL). Latent heat of condensation is released, warming the air and lowering the atmospheric lapse rate, or the rate of temperature change with elevation. As discussed earlier, latent heat exchange is the major energy source that fuels tropical cyclones and hurricanes. It has also been observed that a relation does not necessarily exist between the amount of water vapor and the resulting precipitation over a region. Thus, condensation can occur in cloud formations without the production of precipitation at the ground surface.

Meteorologists use the moisture relationships and the latent-heat concepts to obtain pressure–temperature relationships for cooling of rising moist air in the atmosphere. The rate of temperature change with elevation in the atmosphere is called the **adiabatic lapse rate**. The dry adiabatic lapse rate (DALR) is 9.8°C per km and assumes no phase changes of water. The average ambient lapse rate is about 6.5°C per km, but varies with moisture conditions. An unstable atmosphere is one in which the ambient lapse rate is greater than the DALR. A stable atmosphere is one in which the ambient lapse rate is less than the DALR, and an air parcel tends to cool faster than the environment as it rises vertically. Figure 1–8 shows the variation of lapse rates and different types of atmospheric conditions, with an unstable atmosphere being very conducive to lifting of moist air and to formation of severe weather and/or rainfall conditions.

Mechanisms of Precipitation Formation

Precipitation is the primary input to the hydrologic cycle, whether in the form of rainfall, snow, or hail, and is generally derived from atmospheric moisture. In order for precipitation to occur at the earth's surface,

1. a moisture source must be available,
2. moist air must undergo lifting and resultant cooling,
3. a phase change must occur with resulting condensation onto small nuclei in the air,
4. droplets must grow large enough to overcome drag and evaporation to reach the ground.

Precipitation is often classified according to conditions that generate vertical air motion. Figure 1–9 shows the three main mechanisms:

1. **convective**, due to intense heating of air at the ground, which leads to expansion and vertical rise of air;
2. **cyclonic**, associated with the movement of large air-mass systems, as in the case of warm or cold fronts; and
3. **orographic**, due to mechanical lifting of moist air masses over the windward side of mountain ranges.

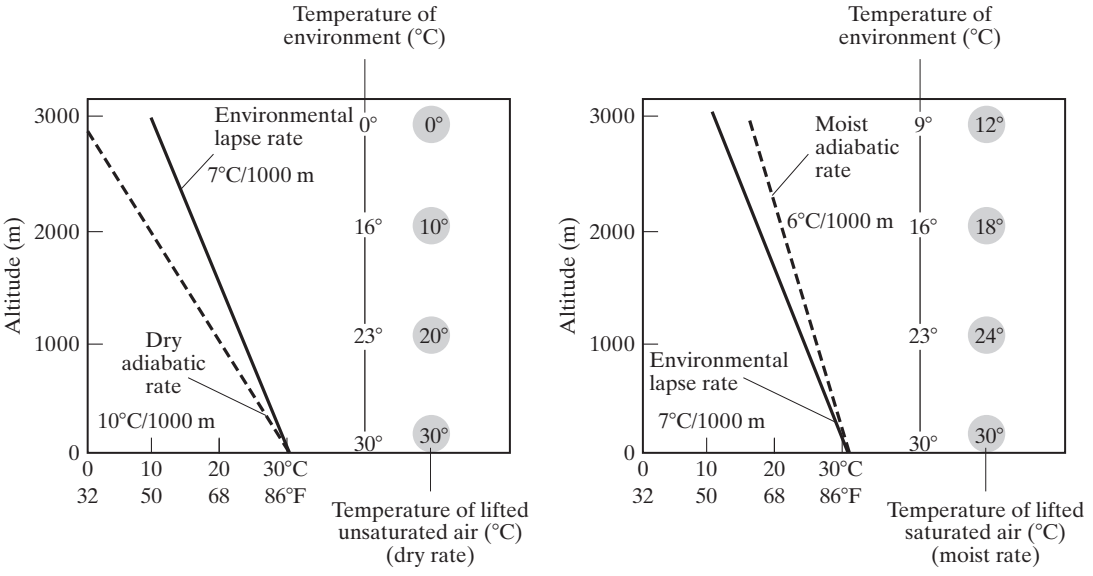

(a) The unsaturated parcel of air at each elevation is colder than its surroundings. The atmosphere is stable with respect to unsaturated, rising air.

(b) The lifted, saturated air parcel is warmer at each elevation than its surroundings. The atmosphere is unstable with respect to saturated, rising air.

Figure 1–8
Variation of lapse rates and different types of atmospheric conditions. When air is colder than its surroundings and rises, it results in what is called a stable atmosphere. On the other hand, when warmer air rises, it results in an unstable atmosphere (greater movement of air).

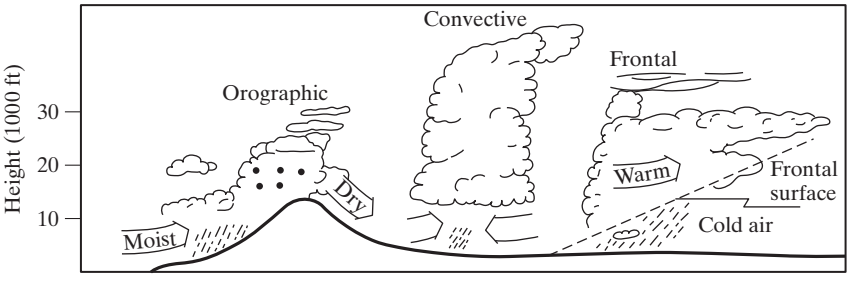

Figure 1–9
The three different precipitation lifting mechanisms that result when air at different temperatures meet in different topographies.

Orographic precipitation is caused by mechanical lifting of moist air over mountain ranges. Notable examples include the western side of the Cascade Mountains, the western side of the Andes in Chile, and the western coast of Norway. On the lee side of mountain barriers are dry areas, called rain shadows, since most of the moisture is dropped as rain or snow over the mountain ranges. Good examples of rain shadows can be found east of the Cascades in Washington and Oregon and east of the Sierra Nevada range in California (see Fig. 1–10). Note that the coastal areas of the United States

receive more rainfall compared to inland areas due to proximity to major moisture sources.

Condensation of water vapor into cloud droplets occurs due to cooling of moist air to a temperature below the saturation point for water vapor. This is most commonly achieved through vertical lifting to levels where pressure and temperature are lower. A large portion of the atmospheric mass lies within 18,000 ft of the surface and contains most of the clouds and moisture. Condensation can be caused by (1) adiabatic cooling (no heat loss to surroundings), (2) mixing of air masses having different temperatures, (3) cooling by advection of cold air masses, and (4) cooling by radiation. Adiabatic cooling is by far the most important producer of appreciable precipitation. Dew, frost, and fog are minor producers of precipitation caused primarily by advective and radiative cooling.

Small condensation nuclei must be present for the formation of cloud droplets. Such nuclei come from many sources, such as ocean salt, dust from clay soils, industrial combustion products, and volcanoes, and they range in size from 0.1 μ to 10 μ. Cloud droplets originally average 0.01 mm in diameter, and it is only when they exceed 0.5 mm that significant precipitation occurs. It may take hours for a small raindrop (1 mm) to grow on a condensation nucleus. As vapor-laden air rises, it cools as it expands; and as saturation occurs, water vapor begins to condense on the most active nuclei.

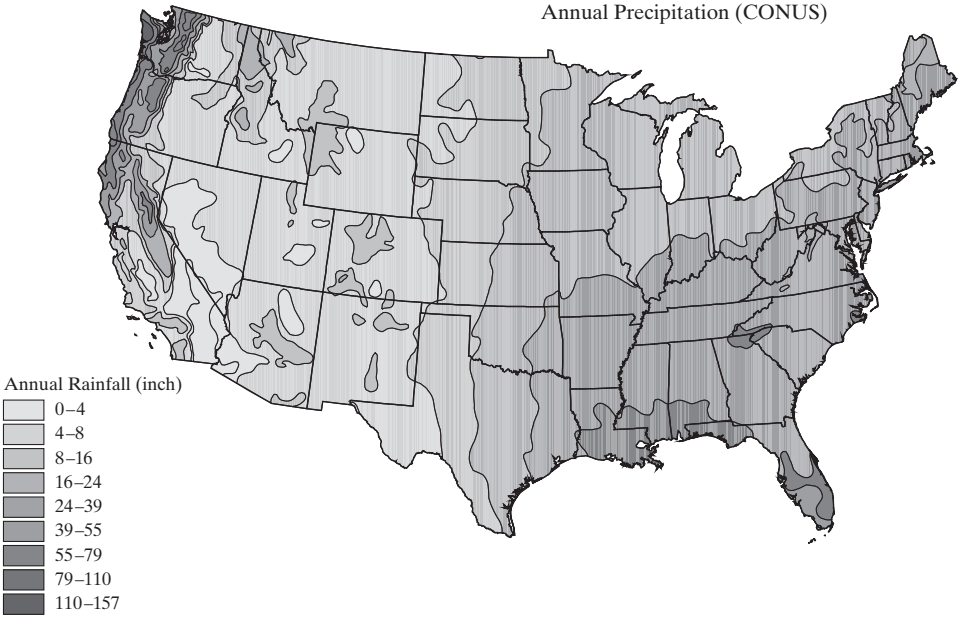

Figure 1–10
Distribution of average annual precipitation across the United States.

The principal mechanism for the supply of water to the growing droplet in early stages is diffusion of water vapor molecules down the vapor-pressure gradient toward the droplet surface. As the droplets increase in mass, they begin to move relative to the overall cloud. However, other processes must support the growth of droplets of sufficient size (0.5–3.0 mm) to overcome air resistance and to fall as precipitation. These include the coalescence process and the ice-crystal process.

The **coalescence process** is considered dominant in summer shower precipitation. As water droplets fall, the smaller ones are overtaken by larger ones, and droplet size is increased through collision. This can produce significant precipitation, especially in warm cumulus clouds in tropical regions. The **ice-crystal process** attracts condensation on freezing nuclei because of lower vapor pressures. The ice crystals grow in size through contact with other particles, and collisions cause snowflakes to form. Snowflakes may change into rain droplets after entering air in which the temperature is above freezing. Snowfall and snowmelt processes are presented in detail in Chapter 2.

1.3 PRECIPITATION

Point Measurement

The main source of moisture for annual rainfall totals is evaporation from the oceans; thus, precipitation tends to be heavier near the coastlines, with distortion due to orographic effects—that is, effects of changes in elevation over mountain ranges. In general, amount and frequency of precipitation is greater on the windward side of mountain barriers (the western side for the United States) and less on the lee side (eastern side), also shown in Figure 1–10. Considerable amounts of precipitation data are available from the NWS, the USGS, and various local governmental agencies. A number of useful websites for precipitation data are listed in Appendix E and on the textbook website http://hydrology.rice.edu. Interpretation of national networks of rainfall data shows extreme variability in space and time, as can be seen in annual and monthly variations in Figures 1–10 and 1–11, respectively. Note the extreme differences in rainfalls between the eastern and western coastlines of the United States.

Time variation of precipitation occurs seasonally or within a single storm, and distributions vary with storm type, intensity, duration, and time of year. Prevailing winds and relative temperature of land and proximity of bordering ocean have an effect. One interesting statistic is the maximum recorded rainfall that can occur at a single gage. These data are shown for eight major U.S. cities in Table 1–1. The highest value for 24-hr rainfall in the United States was 43 in. (1092 mm) in Alvin near Houston, Texas, indicating the impact of severe storms and hurricanes near coastal areas. Some of the greatest rainfall global records for 12 hr to 1 mo periods occur in India and Reunion. These areas are also subject to major flooding.

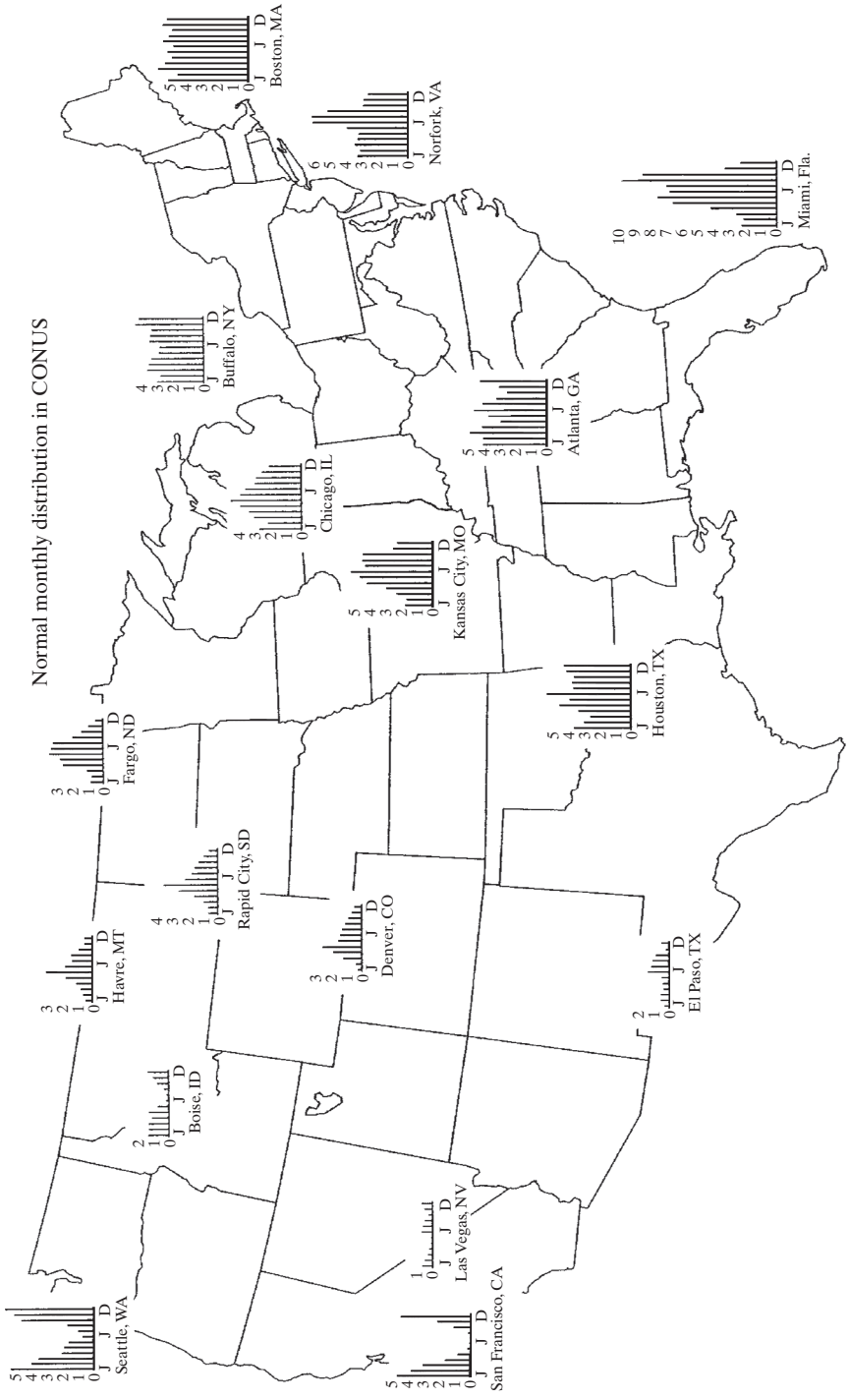

Figure 1–11
Normal monthly distribution of precipitation in different U.S. cities (in.) (1 in. = 25.4 mm). (U.S. Environmental Data Services.)

Table 1–1 Maximum Recorded Rainfall across the United States (in.)

	Duration		
	1 hr	**6 hr**	**24 hr**
San Francisco, CA	1.07	2.34	4.67
Portland, OR	1.31	—	7.66
Denver, CO	2.20	2.91	6.53
St. Louis, MO	3.47	5.82	8.78
New Orleans, LA	4.71	8.62	14.01
Alvin, TX (near Houston)	4.00	15.67	43.00
New York, NY	2.97	4.44	9.55
Miami, FL	4.53	10.64	15.10

Seasonal or monthly distributions for the United States are shown in Figure 1–11, where it is clear that areas such as Florida, California, and the Pacific Northwest have significant seasonal rainfall patterns compared to most areas in the country and along the eastern seaboard. Also, the west and southwest are significantly drier than the east or northwest. But the values shown are deceptive in that high-intensity thunderstorms or hurricanes can produce 15 to 30 in. of rainfall in a matter of days along the Gulf and Atlantic coasts. For example, Oregon and Washington receive most of their rainfall in the winter from fronts that move across the area, whereas in Florida thunderstorms and hurricanes produce large summer totals. Southern California, where most of the population resides, gets significantly less rainfall than the northern part. This difference in available water led to the building of the California Water Project, which transports water hundreds of miles from the reservoirs in the north to the Los Angeles area.

Hourly or 5–15 min variations of rainfall are often important for planning water resource projects, especially urban drainage systems. Figure 1–12 shows the rainfall gage pattern for a major flood in the Houston area from May 2015. Areal rainfalls such as shown in Figure 1–13 from NEXRAD radar sensors are useful in urban hydrologic studies. The intensity and duration of rainfall events and spatial variations are important in determining the hydrologic response for a watershed. Such data are available only from sophisticated rainfall recording networks, usually located in larger urban areas and along major river basins. Rainfall gage networks are maintained by the NWS, the USGS, and local county flood control districts and utilities. An excellent source of rainfall data is now available on specific websites, such as the National Climatic Data Center (NCDC) and the NWS (see Appendix E).

Rainfall gages may be of the recording [Fig. 1–14(a)] or non-recording type, but recording gages are required if the time distribution of rainfall is desired, as is often the case for urban drainage or flood control works. The recording gage operates from a small tipping bucket that records on a data logger, every 0.1 or 0.01 in. of rainfall (or 0.1 or 1 mm in Canada). The data are displayed as a **cumulative mass curve** as in Example 1–2 and can be

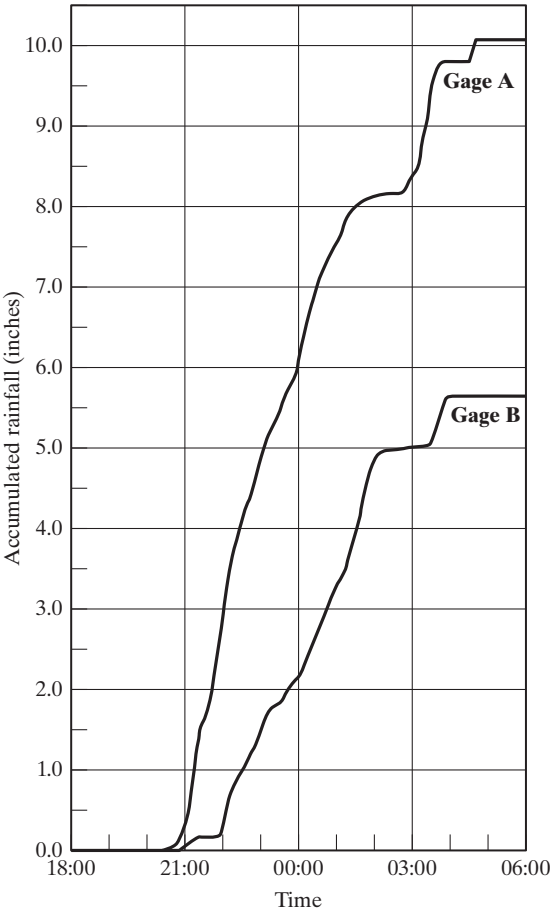

Figure 1–12
Accumulated rainfall for the May 2015 storm event near Houston, Texas.

readily interpreted for total volume and intensity variations. Observers usually report daily or 12-hr amounts of rainfall (in. or mm) for non-recording gages, providing little information on intensity. A typical rainfall and stream gage with telemetry is shown in Figure 1–14(b).

Point rainfall can be plotted as accumulated total rainfall or as rainfall intensity vs. time at a particular gage. A **hyetograph** is a plot of rainfall intensity (in./hr) vs. time, and one is depicted in Example 1–2 along with cumulative mass curves for total rainfall. Hyetographs are often used as input to hydrologic computer models for predicting watershed response to input rainfall.

Statistical methods (Chapter 3) can be applied to a long time series of rainfall data. For example, rainfalls of various duration ranging from 5 min to 24 hr can be analyzed to develop an estimate of, for example, the 100-yr

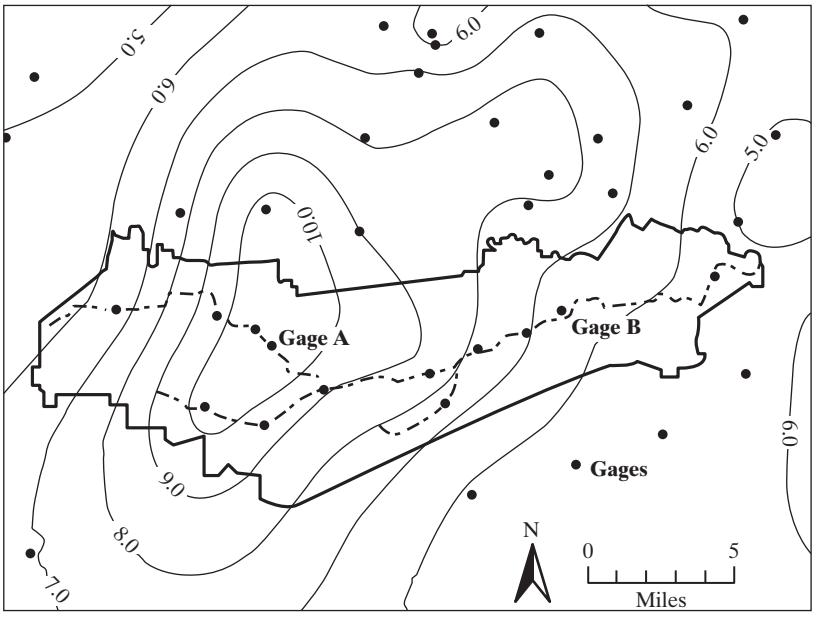

Figure 1–13
May 2015 storm event gage contours (12-hr) for Brays Bayou watershed near Houston, Texas.

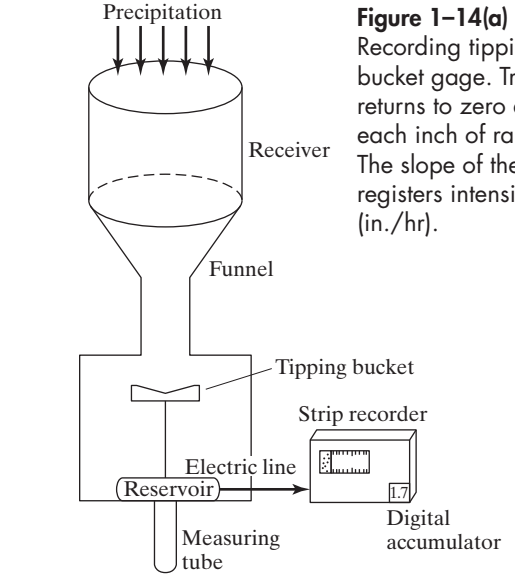

Figure 1–14(a)
Recording tipping bucket gage. Trace returns to zero after each inch of rainfall. The slope of the trace registers intensity (in./hr).

Figure 1–14(b)
Typical recording gage.

EXAMPLE 1–2 **HYETOGRAPHS AND CUMULATIVE PRECIPITATION**

Table E1–2 is a record of precipitation from a recording gage for a storm in Texas, for the period between midnight and 11:15 A.M. on the same day in increments of 0.25 hr. For the data given, develop the rainfall hyetographs and mass curves. Find the maximum-intensity rainfall for the gage in in./hr.

Table E1–2 Rainfall Data from a Recording Gage

Time (hr)	Gage Rainfall (in.)	Gage Intensity (in./hr)	Time (hr)	Gage Rainfall (in.)	Gage Intensity (in./hr)
0	0	0	5.75	3.78	0.24
0.25	0.02	0.08	6	3.84	0.24
0.5	0.07	0.2	6.25	3.9	0.24
0.75	0.4	1.32	6.5	3.95	0.2
1.0	0.55	0.6	6.75	4.1	0.6
1.25	0.6	0.2	7.0	4.3	0.8
1.5	0.62	0.08	7.25	4.93	2.52
1.75	0.62	0	7.5	5.4	1.88
2.0	0.82	0.8	7.75	5.61	0.84
2.25	0.88	0.24	8.0	5.77	0.64
2.5	0.92	0.16	8.25	6.17	1.6

(*continued*)

Table E1–2 (*continued*)

Time (hr)	Gage Rainfall (in.)	Gage Intensity (in./hr)	Time (hr)	Gage Rainfall (in.)	Gage Intensity (in./hr)
2.75	1.06	0.56	8.5	6.22	0.2
3.0	1.1	0.16	8.75	6.27	0.2
3.25	1.47	1.48	9.0	6.29	0.08
3.5	1.87	1.6	9.25	6.3	0.04
3.75	2.32	1.8	9.5	6.31	0.04
4.0	3.1	3.12	9.75	6.32	0.04
4.25	3.4	1.2	10.0	6.33	0.04
4.5	3.48	0.32	10.25	6.34	0.04
4.75	3.54	0.24	10.5	6.35	0.04
5.0	3.62	0.32	10.75	6.36	0.04
5.25	3.68	0.24	11.0	6.37	0.04
5.5	3.72	0.16	11.25	6.38	0.04

SOLUTION

To plot the hyetograph for a gage, we subtract the measurement for each time period from that of the previous time period, and divide by the time step to compute intensity as shown in the table. Because the data are given as a cumulative reading, the mass curves are simply a plot of the data as given (see Fig. E1–2).

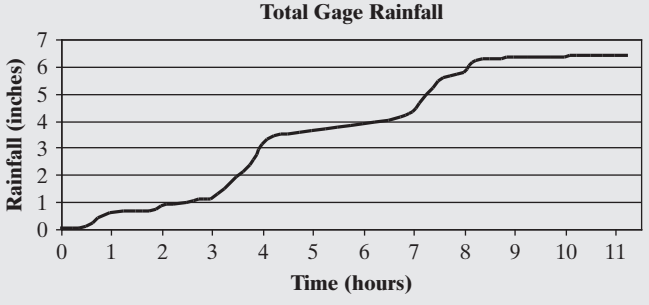

(a)

Figure E1–2(a)
Total gage rainfall and gage rainfall intensity.

The maximum intensity for the gage occurred around 4:00 A.M.

$$\frac{(3.1 - 2.32)\text{ in.}}{0.25\text{ hr}} = 3.12\text{ in./hr}$$

This maximum intensity appears as the tallest bar on the hyetograph and as the region of greatest slope on the cumulative precipitation curve. This

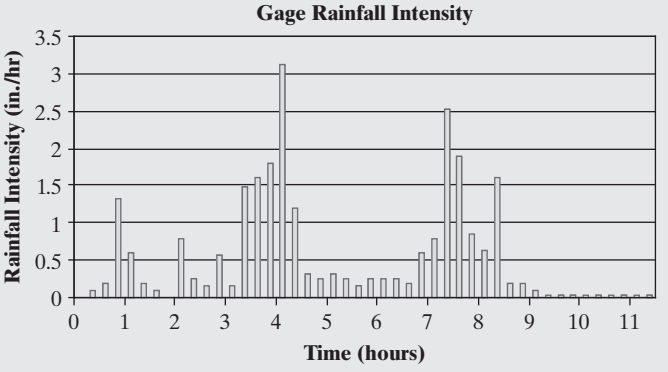

(b)

Figure E1–2(b)

illustrates that the mass curve is the integral of the hyetograph, as, in probability theory, the cumulative distribution function is the integral of the probability density function. Note that the gage had two distinct periods of intense rainfall. These periods of rainfall intensity have the capacity to produce significant runoff and flooding.

frequency event. These data are fitted with a contour line to form one of the curves on the **intensity–duration–frequency** (IDF) curves in Figure 1–15. Other IDF probability lines are derived in a similar fashion for the 2-yr, 5-yr, 10-yr, 25-yr, and 50-yr design rainfalls. It should be noted that IDF curves do not represent the time history of actual storms. Data points on an IDF curve are usually derived from many segments of longer storms, and the values extrapolated by frequency analysis. It can be seen that the intensity of rainfall tends to decrease with increasing duration of rainfall for each of the IDF curves. Instead of analyzing historical rainfall time series, the IDF curves can be used to derive design rainfall events, such as the 10-yr, 2-hr storm, which equals 2.0 in./hr, or the 10-yr, 24-hr storm, which equals 0.3 in./hr or 7.2 in. in 24 hr. One of the homework problems indicates how this procedure is carried out. Such design storms are often used as input to a hydrologic model for drainage design or flood analysis (see Fig. 5–8 and Table 5–9 in Chapter 5).

It is sometimes necessary to estimate point rainfall at a given location from recorded values at surrounding sites. The NWS (1972) has developed a method for this based on a weighted average of surrounding values. The weights are reciprocals of the sum of squares of distances *D,* measured from the point of interest. Thus, for four rain gages where one of them did not record (P1), one would estimate D2, D3, and D4, distances from the non-functional gage. Then the estimate for P1, based on measured values of

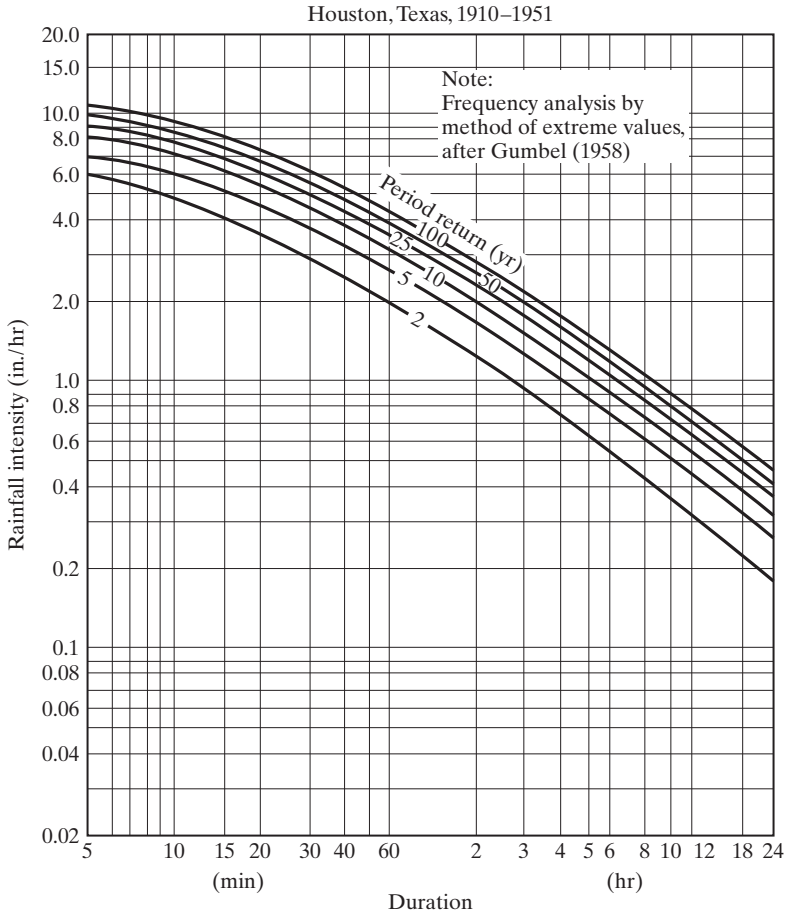

Figure 1–15
Intensity–duration–frequency curves for Houston, Texas.

P2, P3, and P4, would be given by Equation 1–8 below with the weights determined by the inverse square of the distance away from P1.

$$D^2 = x^2 + y^2, \tag{1–6}$$

$$W = 1/D^2 = \text{weight}, \tag{1–7}$$

$$\text{rainfall estimate} = \sum_i P_i W / \sum_i W_i. \tag{1–8}$$

Areal Precipitation

Predicting watershed response to a given precipitation event often requires knowledge of the average rainfall that occurs over a watershed area in a specified duration. The average depth of precipitation over a specific watershed

area is more accurately estimated for an area that is well monitored. Three basic methods exist to derive areally averaged values from point rainfall data: the arithmetic mean, the Thiessen polygon method, and the isohyetal method. Radar-based estimates of rainfall provide an interesting alternative for areas where rainfall gages may be lacking, and these methods are described in Chapter 11.

The simplest method is an **arithmetic mean** of point rainfalls from available gages [Fig. 1–16(a)]. This method is satisfactory if the gages are uniformly distributed and individual variations are not far from the mean rainfall. The method is not particularly accurate for larger areas where rainfall distribution is variable.

The **Thiessen polygon method** [Fig. 1–16(b)] allows for areal weighting of rainfall from each gage. Such a polygon is the locus of points closer to the given gage than to any other. Connecting lines are drawn between

Figure 1–16
The different rainfall averaging methods can produce different results for the same watershed.

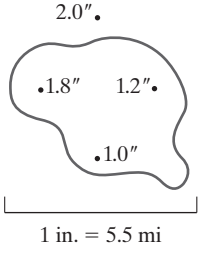

$$\frac{1.8 + 1.2 + 1.0}{3} = 1.33 \text{ in.}$$

(a) Arithmetic mean

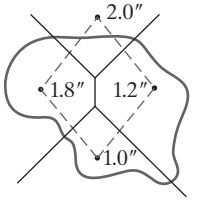

P_i (in.)	A_i (mi^2)	A_i/A_r	$(P_i)(A_i/A_r)$ (in.)
2.0	1.5	0.064	0.13
1.8	7.2	0.305	0.55
1.2	5.1	0.216	0.26
1.0	9.8	0.415	0.42
Σ =	23.6	1.000	1.35 in.

(b) Thiessen polygon method

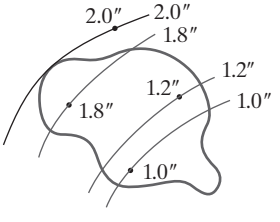

Isohyet (in.)	A (mi^2)	P_{av} (in.)	V (in.$-$mi^2)
2.0	5.1	1.9	9.69
1.8	9.8	1.5	14.7
1.2	3.1	1.1	3.41
1.0	5.6	0.5*	2.8
	23.6		30.6

Average rainfall = 30.6/23.6 = 1.30 in.

* Estimated

(c) Isohyetal method

stations located on a map. Perpendicular bisectors are drawn to form polygons around each gage, and the ratio of the area of each polygon A_i within the watershed boundary to the total area A_T is used to weigh each station's rainfall. The method is unique for each gage network and does not allow for orographic effects (those due to elevation changes), but it is probably the most widely used of the three available methods.

The **isohyetal method** [Fig. 1–16(c)] involves drawing contours of equal precipitation (isohyets) and is the most accurate method. However, an extensive gage network is required to draw isohyets accurately. The rainfall calculation is based on finding the average rainfall between each pair of contours, multiplying by the area between them, totaling these products, and dividing by the total area. The isohyetal method can include orographic effects and storm morphology and can represent an accurate map of the rainfall pattern, as shown for T. S. Allison for a watershed in Houston, TX (see Fig. 1–13).

RAINFALL AVERAGING METHODS **EXAMPLE 1–3**

A watershed covering 28.16 mi^2 has a system of seven rainfall gages, as shown on the map in Figure E1–3(a). Using the total storm rainfall depths given in the accompanying table, determine the average rainfall over the watershed using (a) arithmetic averaging and (b) the Thiessen polygon method.

Gage	Rainfall (in.)
A	5.13
B	6.74
C	9.00
D	6.01
E	5.56
F	4.98
G	4.55

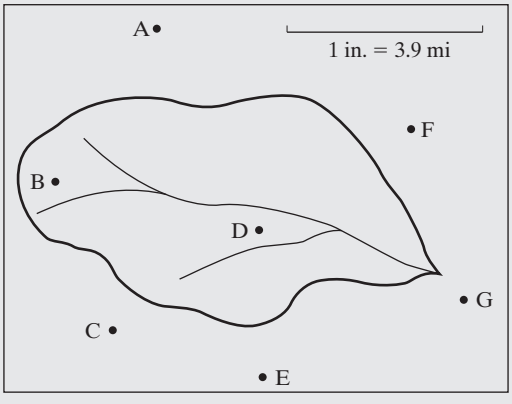

Figure E1–3(a)
Placement of rainfall gages to record rainfall and resulting outflow in the watershed.

SOLUTION

(a) For the arithmetic averaging method, only the gages within the watershed are used—in this example the gages B and D. Thus, the arithmetic average is

$$(6.74 + 6.01)/2 = 6.38 \text{ in.}$$

(b) The first step in the Thiessen polygon method is to connect all nearby rain gages by straight lines. The result is a system of triangles, as shown by the dashed lines in Figure E1–3(b). Next, we construct perpendicular bisectors of the dashed lines in Figure E1–3(c). The bisectors meet at a common point inside or outside the triangle. The resulting polygons around each rainfall gage are known as the Thiessen polygons.

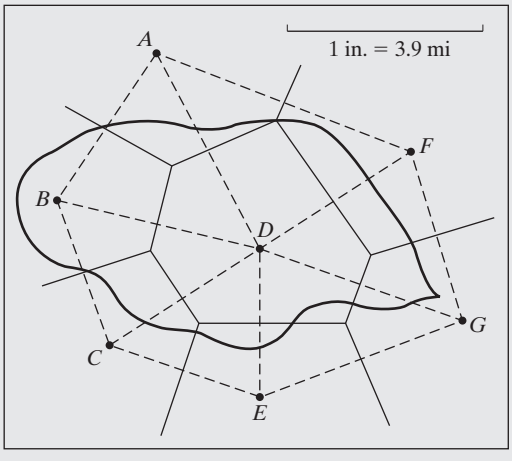

Figure E1–3(b)
Resulting bisectors of rainfall gages to find rainfall in the watershed.

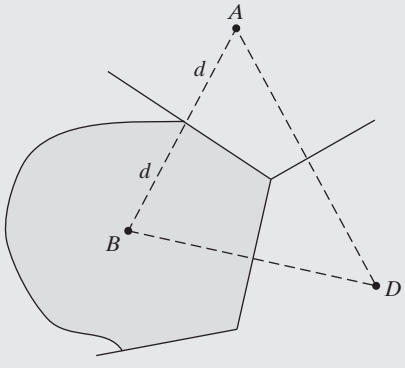

Figure E1–3(c)
Bisectors for the Thiessen polygons.

The area of each polygon within the watershed boundary is measured using a map tool or GIS, or by counting squares on graph paper, and each individual area is divided by the total watershed area and multiplied by the depth of rainfall, measured at its corresponding gage. The sum of fraction area times rainfall for all the gages gives the average rainfall over the watershed. These computations, easily carried out in Microsoft Excel, are shown in the following table. A perpendicular bisector separates the triangle legs into two equal length segments. It intersects the leg at a 90-degree angle. The Thiessen polygons that weigh each rain gage are created by the solid perpendicular bisector lines and the boundary of the watershed.

Thus, the Thiessen polygon method (see Table E1–3) gives an average rainfall over the basin of 6.13 in., compared to 6.38 in. above.

Table E1–3

Gage	P_i (in.)	A_i (mi^2)	A_i/A_t	$(P_i)(A_i/A_t)$ (in.)
A	5.13	1.74	0.062	0.32
B	6.74	6.70	0.238	1.60
C	9.00	1.77	0.063	0.57
D	6.01	13.02	0.463	2.78
E	5.56	0.83	0.029	0.16
F	4.98	2.68	0.095	0.47
G	4.55	1.42	0.050	0.23
		28.16	1.000	6.13

Radar-Based Precipitation

Advances in weather radar (called **NEXRAD** for next-generation radar) in the early 1990s greatly improved our ability to determine rainfall rates over watershed areas. NEXRAD reflects off raindrops in the atmosphere to estimate rainfall rates in time and space. NEXRAD is a 10-cm-wavelength radar that records reflectivity, radial velocity, and spectrum width of reflected signals. A more complete description of radar data products and processing may be found in Chapter 11 and in Crum and Alberty (1993), Klazura and Imy (1993), Smith et al. (1996), Fulton et al. (1998), and Vieux (2004).

Until the advent of the NEXRAD system nationwide, gaging stations were the only source of rainfall data for hydrologic modeling and flood prediction. Radar data can be translated from their original radial coordinates from the source radar into a gridded coordinate system with 1.0-km^2 resolution grids. Recent efforts have been successful in measuring rainfall rates and cumulative totals using radar technology developed and implemented in the 1990s (Vieux and Bedient, 1998; Bedient et al., 2000, 2003; Vieux, 2004). Figure 1–17 depicts the type of radar rainfall information available from NEXRAD radar systems every 5–6 minutes for a storm event in Louisiana. Chapters 10 and 11 present the background and details for using radar data to support hydrologic prediction from models and for associated flood alert systems.

1.4 THE HYDROLOGIC CYCLE

The hydrologic cycle is a very complex series of processes [Fig. 1–1(b)], but under certain well-defined conditions the response of a watershed to rainfall, infiltration, and evaporation can be calculated if simple assumptions can be made. A **watershed** is a contiguous area that drains to an outlet, such that precipitation that falls within the watershed runs off through

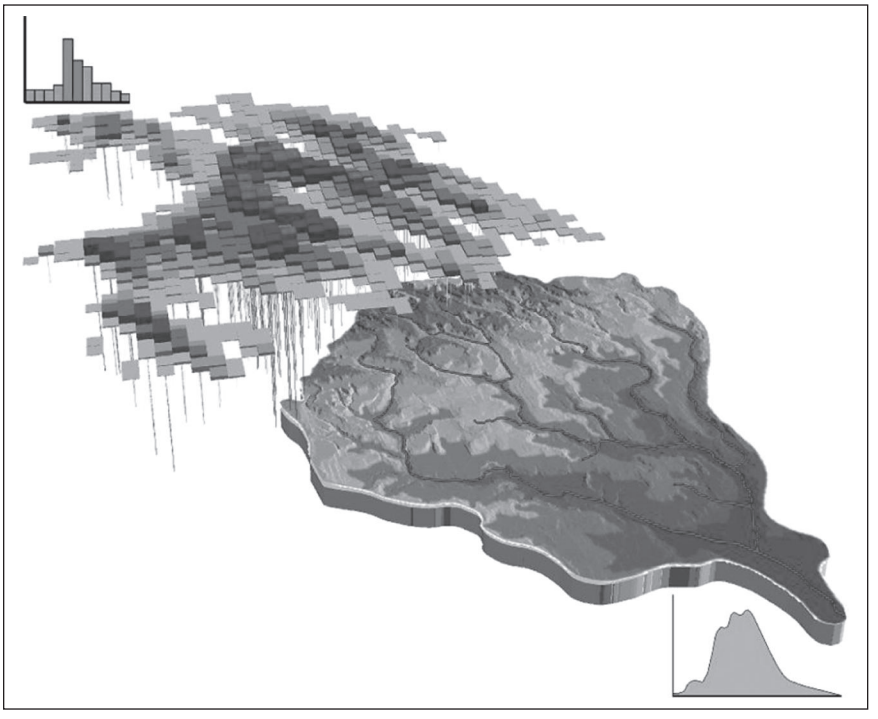

Figure 1–17
Graphical representation for NEXRAD rainfall data over a watershed located in central Louisiana.

that single outlet (the term **catchment** is sometimes used synonymously for just the surface portion of the watershed). For example, if the rainfall rate over a watershed area is less than the rate of infiltration into soil and if there is ample storage in soil moisture, then direct runoff from the surface and resulting streamflow will be zero. If, on the other hand, antecedent or previous rainfall has filled soil storage and if the rainfall rate is so large that infiltration and evaporation can be neglected, then the volume of surface runoff will be equal to the volume of rainfall. In most cases, however, the conditions fall somewhere between these limitations, and we must carefully measure or calculate more than one component of the cycle to predict watershed response. The watershed is the basic hydrologic unit within which all measurements, calculations, and predictions are made in hydrology (see Fig. 1–13).

The Water Balance

The basic components of the hydrologic cycle include precipitation, evaporation, evapotranspiration, infiltration, overland flow, streamflow, and

ground water flow [Fig. 1–1(a)]. The movement of water (rainfall and runoff) through various phases of the hydrologic cycle varies greatly in time and space, giving rise to extremes of floods or droughts. The magnitude and the frequency of occurrence of these extremes are of great interest to the engineering hydrologist from a design and operations standpoint. In some cases, it is possible to perform a water budget calculation in order to predict changes in storage to be expected based on inputs and outputs from the system.

For any hydrologic system, a water budget can be developed to account for various flow pathways and storage components. The hydrologic continuity equation for any system is

$$I - Q = \frac{dS}{dt}, \tag{1–9}$$

where

I = inflow in L^3/t
Q = outflow in L^3/t,
dS/dt = change in storage per time in L^3/t.

The simplest system is an impervious inclined plane, confined on all four sides with a single outlet. A small urban parking lot follows such a model, and as rainfall accumulates on the surface, the surface detention, or storage, slowly increases and eventually becomes outflow from the system. Neglecting evaporation for the period of input, and assuming a long rainfall time period, all input rainfall eventually becomes outflow from the area, but delayed somewhat in time. The difference between inflow to the parking lot and outflow at any time represents the change in storage [Eq. (1–9)]. Thus, the total storage volume that is eventually released from the area is equal to the accumulated difference in inflow volume and outflow volume, or $\int (I - Q)\Delta t$.

The same concept can be applied to small basins or large watersheds. Note that urban watersheds include both natural and man-made elements. For a given time period, a conceptual mathematical model for the budget for the urban hydrologic cycle shown in Figure 1–18 would become, in units of depth (in. or mm) over the basin,

$$P - R - G - E - T = \Delta S, \tag{1–10}$$

where

P = precipitation,
R = surface runoff,
G = ground water flow,

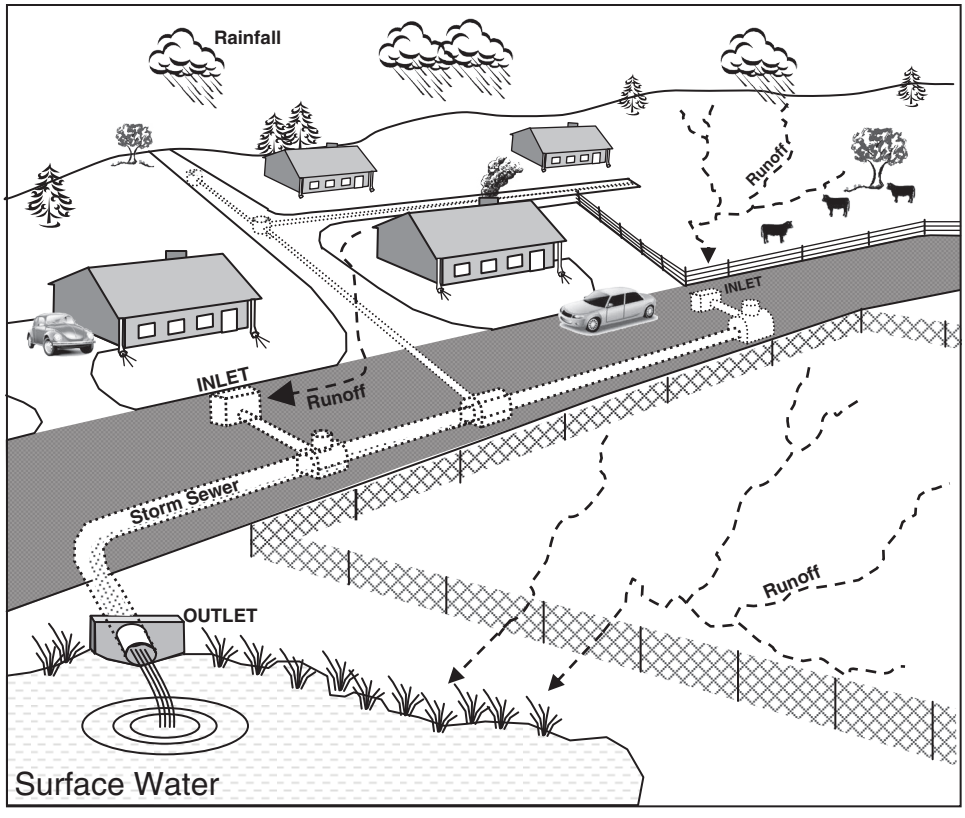

Figure 1–18
Urban hydrologic cycle. A combination of runoff from natural surroundings and man-made drainage systems, these runoffs come together at a single outlet.

E = evaporation,
T = transpiration,
ΔS = change in storage in a specified time period.

A **runoff coefficient** can be defined as the ratio R/P for any watershed. Note that infiltration I is a loss from the surface system and a gain to ground water, and thus cancels out of the overall budget above. Also, the units of inches (or mm) represent a volume of water when multiplied by the surface area of the watershed. If a water body receives inflow for a period of time, the change in water depth due to the inflow can be easily calculated. There are two ways of denoting the volume of water that is added, either as a flow rate for a specified time or as a water depth across an area. The following equation results:

$$\text{volume} = (\text{flow rate})(\text{time}) = (\text{depth})(\text{watershed area}). \quad (1\text{–}11)$$

Typical units may be English or metric, as indicated below:

flow rate	cfs or m^3/s
time	seconds, days, months
depth	in. or mm
area	acres, sq mi, or sq km

To convert from a flow to a change in water depth, rearrange the equation above and multiply by necessary conversion factors:

$$\text{depth} = \frac{(\text{flow rate})(\text{time})(\text{conversion factor})}{\text{watershed area}}. \qquad (1\text{–}12)$$

Conversion factors = (30 days/month) (24 hr/day) (3600 s/hr) (1 acre/43,560 ft) (12 in./ft). Note that **1.0 ac-inch = 1.008 cfs-hr.**

WATER BALANCE IN A LAKE **EXAMPLE 1–4**

For a given month, a 300-acre lake has 15 cfs of inflow, 13 cfs of outflow, and a total storage increase of 16 ac-ft. A USGS gage next to the lake recorded a total of 1.3 in. precipitation for the lake for the month. Assuming that infiltration loss is insignificant for the lake, determine the evaporation loss, in inches, over the lake for the month.

SOLUTION

Solving the water balance for inflow I and outflow O in a lake gives, for evaporation,

$$\underset{\text{evaporation}}{E} = \underset{\text{inflow}}{I} - \underset{\text{outflow}}{O} + \underset{\text{precipitation}}{P} - \underset{\text{change in storage}}{\Delta S},$$

$$I = \frac{(15\ \text{ft}^3/\text{s})(\text{ac}/43{,}560\ \text{ft}^2)(12\ \text{in./ft})(3600\ \text{s/hr})(24\ \text{hr/day})(30\ \text{day/month})(1\ \text{month})}{300\ \text{ac}}$$

$$= 35.70\ \text{in.},$$

$$O = \frac{(13\ \text{ft}^3/\text{s})(\text{ac}/43{,}560\ \text{ft}^2)(12\ \text{in./ft})(3600\ \text{s/hr})(24\ \text{hr/day})(30\ \text{day/month})(1\ \text{month})}{300\ \text{ac}}$$

$$= 30.94\ \text{in.},$$

$$P = 1.3\ \text{in.},$$

$$\Delta S = \frac{(16\ \text{ac} - \text{ft})(12\ \text{in./ft})}{300\ \text{ac}} = 0.64\ \text{in.},$$

$$E = (35.70) - (30.94) + (1.3) - (0.64)\ \text{in.},$$

$$E = 5.42\ \text{in.}$$

EXAMPLE 1–5 **WATER BALANCE IN A SWIMMING POOL**

A swimming pool (20 ft × 20 ft × 5 ft) has a small leak at the bottom. You are given measurements of rainfall, evaporation, and water level on a daily basis for 10 days. As an engineer, use the water balance to determine the average daily leakage out of the swimming pool in ft^3/day. Assume the pool is exactly 5 ft (60 inches) deep at the end of day 1.

Day	Evaporation (in.)	Rainfall (in.)	Measured Level (in.)
1	0.5		60
2	0	1.0	
3	0.5		
4	0	2.0	
5	0.5		
6	0.5		
7	0	4.0	
8	0.5		
9	0.5		
10	0.5		52

SOLUTION

The water-balance equation becomes:

$$\text{outflow} = \text{precipitation} - \text{evaporation} - \Delta\text{storage}$$

All values must be in the same units. Thus, the total change in storage is $52 - 60 = -8$ in. The precipitation is $1.0 + 2.0 + 4.0 = 7$ in. The evaporation is $(7)(0.5) = 3.5$ in.

Thus,

$$\text{outflow} = 7 - 3.5 - (-8),$$

$$\text{outflow} = 11.5 \text{ in.}$$

Outflow should be in ft^3/day. The height change is distributed over the pool area.

$$\text{outflow} = \frac{(11.5 \text{ in.})(1 \text{ ft}/12 \text{ in.})(20 \text{ ft})(20 \text{ ft})}{10 \text{ days}},$$

$$\text{outflow} = 38.3 \text{ ft}^3\text{day}.$$

The Watershed

The watershed or basin area is an important physiographic property that determines the volume of runoff to be expected from a given rainfall event that falls over the area. Watershed areas vary in size from a few acres in an urban area to thousands of square miles for a major river basin. The **watershed divide** is the loci of points (the ridge line) that separates two adjacent watersheds, which

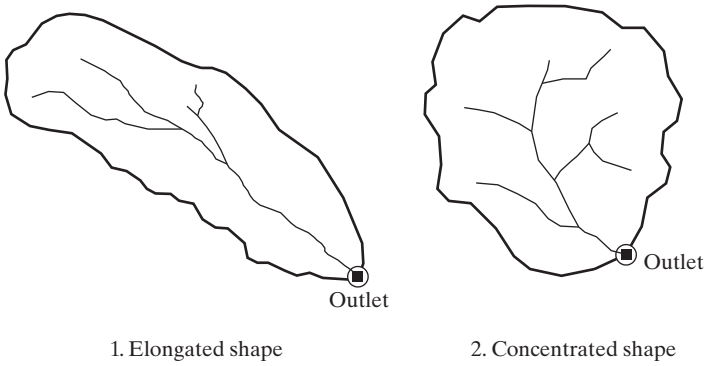

Figure 1–19(a)
Typical watershed area shapes. The difference in shape affects timing and peak flow of runoff to the outlet.

then drain into two different outlets. Figure 1–19(a) depicts several watershed areas that have been defined based on topographic or elevation data.

The topographic divide for a basin is usually drawn on a USGS map or quadrangle sheet (1:24,000 scale) or other topographic map by identifying high points and contours of constant elevation to determine directions of surface runoff. The area encompassed by the divide is the watershed area. Runoff originates at higher elevations and moves toward lower elevations in a direction perpendicular to the contour lines, as shown in Figure 1–19(b). Note that the arrows indicate the directions of flow in each

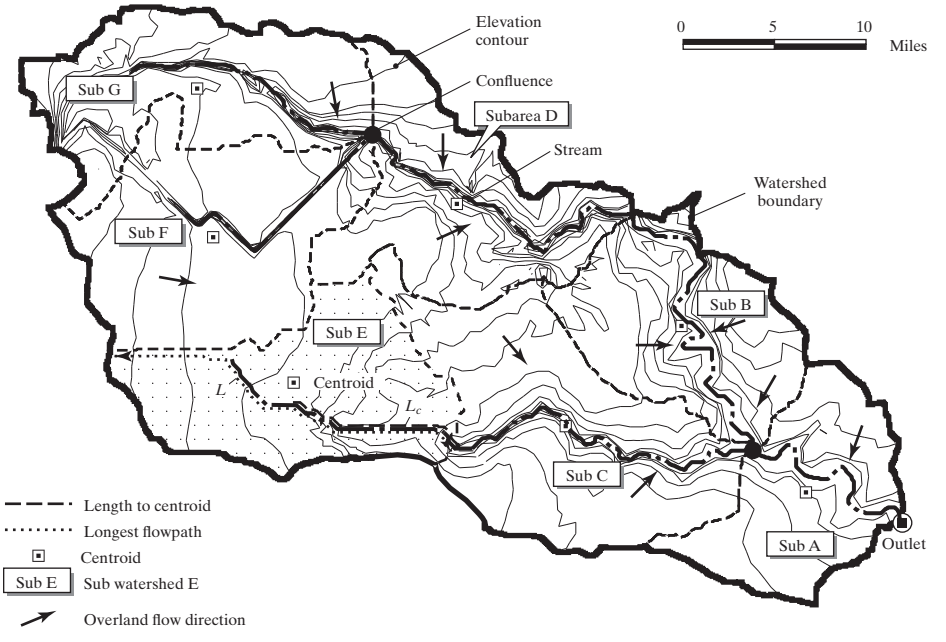

Figure 1–19(b)
Subwatershed delineation with overland flow direction and elevation contours.

subarea (A through G), and that flows generally move toward the nearest stream in a down-gradient direction. This is described in more detail in Section 1.7.

In general, the larger the watershed area, the greater the surface runoff rate, the greater the overland flow rate, and the greater the streamflow rate. Formulas developed to relate peak flow to watershed area take the form $Q_p = cA^n$, where Q_p = peakflow, A = watershed area, and c and n are regression constants to be determined (Chapter 3). Peak flow is the product of a channel cross-sectional area and its average velocity at peak conditions. Watershed area is an important parameter that governs peak flow in most of the hydrologic prediction methods described later in this chapter and throughout the text.

Watershed relief is the elevation difference between two reference points within a watersehed. Maximum relief is the difference between the highest point on the watershed divide and the watershed outlet. The longitudinal profile of the main channel is a plot of elevation vs. horizontal distance and is an indicator of channel gradient. Most streams, and especially rivers, show a decrease in channel gradient as one proceeds in a downstream direction [see Fig. 1–19(b)]. This is due to the interaction of bottom friction and water depth. Channel gradients vary from about 0.1 (10%) for a mountain stream and as low as 0.0001 (.01%) for coastal areas.

1.5 SIMPLE RAINFALL–RUNOFF

Hydrologists are concerned with the amount of surface runoff generated in a watershed for a given rainfall pattern, and attempts have been made to analyze historical rainfall, infiltration, evaporation, and streamflow data to develop predictive relationships. When rainfall exceeds the infiltration rate at the surface, excess water begins to accumulate as surface storage in small depressions governed by surface topography. Eventually, the entire area is contributing to runoff at the outlet of a watershed.

The USGS as well as local flood control agencies are responsible for extensive hydrologic gaging networks within the United States, and data gathered on an hourly or daily basis can be plotted for a given watershed to relate rainfall to direct runoff for various time periods. Annual rainfall–runoff relationships remove seasonal effects and other storage effects, so that the relationship of rainfall minus losses vs. runoff can often be approximated by a linear regression line. The USGS developed a series of reports and relationships for predicting flood-peak discharges for urban and rural areas in the United States. Some of these are reviewed in Chapter 3.

Simple rainfall–runoff relationships should be used in water resources planning studies only where approximate water balances are required. A detailed knowledge of the magnitude and time distribution of both rainfall and runoff or streamflow is required for most flood control or floodplain studies, especially in urban watersheds. Many websites listed in Appendix E support USGS streamflow data from most of the stations in the United States.

One of the simplest rainfall–runoff formulas, which is often used for drainage design purposes in small watersheds and/or basins, is the **Rational Method** (Chapters 6 and 9), which allows for the prediction of peak flow Q_p (cfs) from the formula

$$Q_p = CiA, \tag{1–13}$$

where

C = runoff coefficient, variable with land use,
i = intensity of rainfall of chosen frequency for a duration equal to time of concentration t_c (in./hr),
t_c = equilibrium time for rainfall occurring at the most remote portion of the basin to contribute flow at the outlet (min or hr),
A = area of watershed (acres).

The Rational Method is usually attributed to Kuichling (1889) and Lloyd-Davies (1906), but Mulvaney (1851) clearly outlined the procedure in a paper in Ireland. The underlying assumption is that a steady, uniform rainfall rate will produce maximum runoff when all parts of a watershed are contributing to outflow, a condition that is met after the time of concentration t_c has elapsed. Time of concentration t_c is defined as the time for a wave of water to propagate from the most distant point in the basin to the outlet (see Section 2.1). Runoff is assumed to reach a maximum when the rainfall intensity lasts as long as the t_c. The runoff coefficient is assumed constant during a storm event. More details can be found in later chapters and in McCuen (2005). The rational method is often used in small urban areas to design drainage systems, including pipe systems, culverts, and open channels. Chapters 6 and 9 present detailed discussion and examples of the rational method applied to small watershed areas. Larger watersheds (greater than a few square miles) usually require a consideration of the entire hydrograph because timing and storage issues become important, and the rational method is usually limited to basins less than a few hundred acres in size.

1.6 STREAMFLOW AND THE HYDROGRAPH

The hydrologic cycle is shown as a schematic in Figure 1–1, where precipitation P initially falls on the land surface, and it may distribute to fill **depression storage**, infiltrate to become soil moisture and shallow ground water, or travel as interflow to a receiving stream. Evaporation E is often a small component of a specific storm event, since it is minimal as rain is actually falling, and is usually only a factor in longer-term water balances. Depression storage capacity is usually satisfied early in storm passage, followed by infiltration capacity into the soil (see Fig. 1–20). Eventually, overland flow and surface runoff commence after soil storage and depression storage are satisfied. Overland flow then quickly moves down-gradient toward the nearest small rivulet or channel, which then flows into the next larger stream, and eventually reaches the main stream channel as open-channel flow.

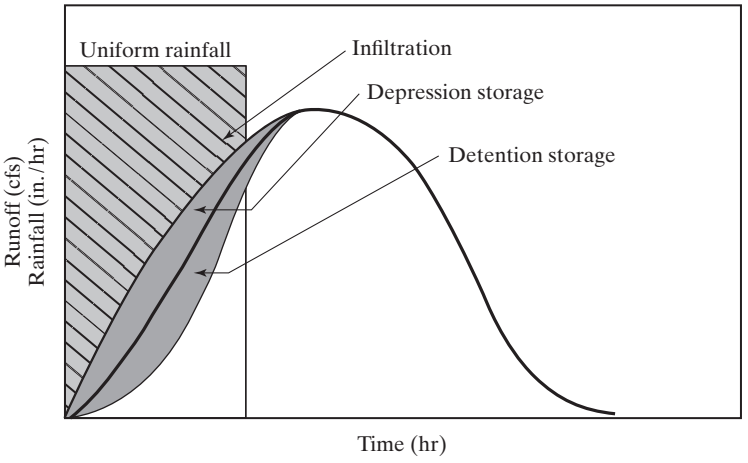

Figure 1–20
Distribution of uniform rainfall presented with a runoff hydrograph. Note the parameters of infiltration, depression storage, and detention storage.

The **hydrograph**, a plot of flow rate vs. time that is measured at a stream cross section, is made up primarily of various contributing flows. Base flow can also contribute and is produced from soil moisture and ground water contributions. The actual shape and timing of the hydrograph is determined largely by the size, shape, slope, and storage in the basin and by the intensity and duration of input rainfall. Chapter 2 presents these concepts in more detailed examples for ultimate hydrograph analysis. Evaporation and infiltration losses are covered briefly in Section 1.8, and in more detail in Chapter 2.

The classic concept of streamflow generation by **overland flow** is due to Horton (1933), who proposed that overland flow is common and areally widespread. Later investigators incorporated concepts of heterogeneity, which exists across natural watersheds, and developed the partial area contribution concept (Betson, 1964). This model recognized that only certain portions of a watershed regularly contribute overland flow to streams and that no more than about 10% of a watershed contributes overland flow. In urban environments with large areas of impervious cover, the overland flow percentage may be larger. Significant surface runoff occurs only after rainfall intensity exceeds infiltration capacity, or ($i > f$) and soil moisture storage has been filled. Infiltration f is the loss rate into the soil system.

The channel may contain a certain amount of **base flow** coming from ground water and soil contributions even in the absence of rainfall. Discharge from rainfall excess, after infiltration losses have been subtracted, makes up the **direct-runoff hydrograph (DRO)**. The total storm hydrograph consists of direct runoff plus base flow. The duration of rainfall determines the portion of watershed area contributing to the peak, and the intensity of rainfall determines the resulting peak flow rate. If rainfall maintains a constant intensity for a very long time, maximum storage is achieved and a state of equilibrium discharge is reached, where the hydrograph tends to